

version of May 8, 2012

Wedges, Cones, Cosmic Strings, and the Reality of Vacuum Energy

S. A. Fulling^{1,2}, C. S. Trendafilova^{1,2}, P. N. Truong^{1,2,3},
J. Wagner^{1,4}

¹ Department of Mathematics, Texas A&M University, College Station, TX,
77843-3368 USA

² Department of Physics and Astronomy, Texas A&M University, College Station,
TX, 77843-4242 USA

³ Present address: Department of Physics, University of California, Berkeley, CA,
94720-7300 USA

⁴ Present address: Department of Physics and Astronomy, University of California,
Riverside, CA, 92521 USA

E-mail: fulling@math.tamu.edu

Abstract. One of J. Stuart Dowker's most significant achievements has been to observe that the theory of diffraction by wedges developed a century ago by Sommerfeld and others provided the key to solving two problems of great interest in general-relativistic quantum field theory during the last quarter of the twentieth century: the vacuum energy associated with an infinitely thin, straight cosmic string, and (after an interchange of time with a space coordinate) the apparent vacuum energy of empty space as viewed by an accelerating observer. In a sense the string problem is more elementary than the wedge, since Sommerfeld's technique was to relate the wedge problem to that of a conical manifold by the method of images. Indeed, Minkowski space, as well as all cone and wedge problems, are related by images to an infinitely sheeted master manifold, which we call Dowker space. We review the research in this area and exhibit in detail the vacuum expectation values of the energy density and pressure of a scalar field in Dowker space and the cone and wedge spaces that result from it. We point out that the (vanishing) vacuum energy of Minkowski space results, from the point of view of Dowker space, from the quantization of angular modes, in precisely the way that the Casimir energy of a toroidal closed universe results from the quantization of Fourier modes; we hope that this understanding dispels any lingering doubts about the reality of cosmological vacuum energy.

PACS numbers: 03.70.+k, 41.20.Cv

AMS classification scheme numbers: 81T55, 34B27, 81Q05

1. Introduction

1.1. Basics

A *wedge* is a region $\Omega \subset \mathbf{R}^3$ bounded by two intersecting planes on which, say, the Dirichlet boundary condition is imposed. All the standard linear partial differential equations (wave, heat, Schrödinger, resolvent, ...) for all the standard fields (scalar, electromagnetic, spinor, ...) can be studied there, and their respective Green functions constructed, by standard but not totally trivial methods.

As the prototype of a wedge problem we consider the conditions defining the “cylinder kernel”, which provides [1, 2, 3, 4] the most direct way of calculating the vacuum expectation value of the energy of a quantized massless scalar field:

$$T(t, \mathbf{x}, \mathbf{x}') \quad \text{is defined in } \mathbf{R}^+ \times \Omega \times \Omega, \quad (1)$$

$$\frac{\partial^2 T}{\partial t^2} = -\nabla^2 T \quad \text{for } \mathbf{x} \text{ in } \Omega, \quad (2)$$

$$T(t, \mathbf{x}, \mathbf{x}') = 0 \quad \text{for } \mathbf{x} \text{ in } \partial\Omega, \quad (3)$$

$$T(0, \mathbf{x}, \mathbf{x}') = \delta(\mathbf{x} - \mathbf{x}') \quad \text{for } \mathbf{x} \text{ in } \Omega, \quad (4)$$

$$T(t, \mathbf{x}, \mathbf{x}') \quad \text{is bounded as } t \rightarrow +\infty. \quad (5)$$

Explicitly, in the three-dimensional case, we have

$$\Omega = \{(r, \theta, z): 0 < r < \infty, 0 < \theta < \theta_0, -\infty < z < \infty\}, \quad (6)$$

$$\nabla^2 = \frac{\partial^2}{\partial r^2} + \frac{1}{r} \frac{\partial}{\partial r} + \frac{1}{r^2} \frac{\partial}{\partial \theta^2} + \frac{\partial^2}{\partial z^2}, \quad (7)$$

$$\delta(\mathbf{x} - \mathbf{x}') = \frac{1}{r} \delta(r - r') \delta(\theta - \theta') \delta(z - z'), \quad (8)$$

and an additional implied boundary condition,

$$T(t, \mathbf{x}, \mathbf{x}') \quad \text{is bounded as } z \rightarrow \pm\infty. \quad (9)$$

Often the two-dimensional reduction is of interest:

$$\Omega = \{(r, \theta): 0 < r < \infty, 0 < \theta < \theta_0\}, \quad (10)$$

$$\nabla^2 = \frac{\partial^2}{\partial r^2} + \frac{1}{r} \frac{\partial}{\partial r} + \frac{1}{r^2} \frac{\partial}{\partial \theta^2}, \quad (11)$$

$$\delta(\mathbf{x} - \mathbf{x}') = \frac{1}{r} \delta(r - r') \delta(\theta - \theta'). \quad (12)$$

Remarks: The corresponding Green function for all of \mathbf{R}^3 in the role of Ω is

$$T_0(t, \mathbf{x}, \mathbf{x}') = \frac{t}{\pi^2(t^2 + |\mathbf{x} - \mathbf{x}'|^2)^2}. \quad (13)$$

It is proportional to the t -derivative of the fundamental solution of the Laplacian in \mathbf{R}^4 , with $t' = 0$. It follows that the most relevant dimension is 4, the same as the space-time dimension of the quantum field theory, and we henceforth revise our terminology

accordingly. It is important to understand that in the cylinder-kernel formalism, t is “imaginary” time, related to the physical time x^0 by $it = x^0 - x^{0'}$. The term “cylinder kernel” refers to the domain $\mathbf{R}^+ \times \Omega$ in \mathbf{R}^4 , not to the cylindrical character of Ω itself in the present work.

The angle θ_0 is “good” if $\theta_0 = \pi/N$ for some integer N . In other words, the wedge considered is one of $2N$ equal sectors into which Euclidean space is divided. (For mixed boundary conditions (Neumann on one side and Dirichlet on the other), θ_0 is good only if N is even (the number of sectors is a multiple of 4).) In such a case the problem can be solved immediately by the method of images: Replicate the singular source (8) by perpendicular reflection of \mathbf{x}' through each boundary plane, with a minus sign for the Dirichlet condition but a plus for Neumann. Continue the construction through all $2N$ sectors; the two directions of continuation meet consistently. The solution of the PDE in \mathbf{R}^3 with this multiple source is easily constructed as a linear combination of copies of T_0 with its source moved to each of the images. That function satisfies the desired boundary condition on each plane, so its restriction to Ω is the desired Green function T .

If the angle is “bad”, the replicated wedges cannot match up to constitute Euclidean space. The constructed covering space is a *cone*, which is locally flat but has a singularity at the axis. The circumference of a circle centered at the axis is θ_1 times the radius, where θ_1 is θ_0 times the number of sectors in the construction. (The number of sectors in such a case is not uniquely determined. One could either take the simplest case, two sectors, or choose the value that makes θ_1 closest to 2π .) To solve a wedge with a bad angle by images, therefore, one must know the cylinder kernel for the related problem on the cone. The latter satisfies the same equations (2), (4), (5), (9) (Ω now being the cone manifold), but the boundary condition (3) is replaced by the periodicity condition

$$T(t, r, \theta + \theta_1, z, \mathbf{x}') = T(t, r, \theta, z, \mathbf{x}'), \quad \frac{\partial T}{\partial \theta}(t, r, \theta + \theta_1, z, \mathbf{x}') = \frac{\partial T}{\partial \theta}(t, r, \theta, z, \mathbf{x}'). \quad (14)$$

Once this Green function has been found, it can be used in the role of T_0 to construct the T for the wedge.

In both cone and wedge, there is a technical issue about uniqueness of the solution, which is resolved by choosing the solution of minimal growth as the axis is approached [5, 6].

1.2. History

At the end of the 19th century Sommerfeld [7, 8, 9, 10] used the method of images to solve the problem of diffraction of waves by edges and wedges. (The seminal paper [7] has been translated with extensive commentary in [11].) His and most other early work was concerned with the wave equation and with the solution corresponding to a particular incident wave, but of course the foregoing remarks about boundary conditions and images also apply there. At that time it was natural to think of the cone as a Riemann surface in the sense of complex analysis, rather than a locally flat Riemannian manifold

in the sense of differential geometry. Therefore, initially only values of θ_1 of the form $2\pi M$ were considered, and hence wedges of angles $\theta_0 = \pi M/N$. Sommerfeld [7] was primarily concerned with a sharp edge (conducting half-plane), for which $\theta_0 = 2\pi$ and hence a 2-sheeted Riemann surface ($\theta_1 = 4\pi$) divided into two sectors ($N = 1$) suffice. He gave mere indications of how to treat the general case $\theta_0 = \pi M/N$, but his method was made explicit by Carslaw [12], and the case of a right-angle wedge ($\theta_0 = \frac{3\pi}{2}$, three sheets, four sectors) was worked out in detail by Reiche [15]. (The case $2\pi - \theta_0 = \frac{\pi}{3}$, $M = 5$, $2N = 6$, is treated in the notes to [11].) Sommerfeld [7, pp 346–347, 357] also showed how to construct solutions on an infinite-sheeted Riemann surface, but did not really explain how to use them to solve the original problem for $\theta_0 \neq \pi M/N$ (and the commentators in [11] describe this passage as “surrealistic”). He gave an explicit, though still very brief, prescription in [9, p 38], as cited in Carslaw [14], and Wiegrefe [16] gave a more thorough treatment.

Sommerfeld constructed solutions on Riemann surfaces by conformal mappings from the complex plane, but then he represented them by certain contour integrals, which are periodic with period θ_1 . Carslaw [13, 14] noted that these integrals continue to satisfy the desired differential equations and periodicity even when θ_1/π is not rational. Knowing this, it is possible to dispense with the Riemann surfaces and obtain the solution of the wedge problem — for arbitrary $\theta_0 = \frac{1}{2}\theta_1$ — from this periodic function by adding a single image term. Carslaw’s papers [12, 13, 14] are also notable for emphasizing the generality of the method, beyond the wave equation. Other work on wedge problems during this era is reviewed in the introduction to [17], which also constructs Green functions for the wave equation for arbitrary θ_0 in terms of standard special functions, without relying on either Riemann surfaces or contour integral representations. See also [18, 19, 20] for applications of concepts of scattering and diffraction theory.

Until 1977 the mathematically simpler problem of a cone was thought of by physicists merely as a means to the end of solving the problem of a wedge; it would never have occurred to Sommerfeld to speak of a “cosmic string”, for example. But Stuart Dowker was well versed in this classic literature, and he realized that it could be instantly applied to problems that had arisen in quantum field theory in curved space-time [21, 22, 23, 24, 25]. Again, the simplest problem was originally seen as a tool for studying something more recondite: In [21, 22] the emphasis is on the analytic continuation of a cone manifold to “Rindler space”, the space-time visible to a uniformly accelerated observer; the periodicity is in the (imaginary) time coordinate and represents the effective temperature of the vacuum state. (In lieu of a long list of references, we refer to a previous review article [26].) Ten years later, however, the cone as a spatial manifold came to be regarded as physically realistic, as the idealized zero-radius limit of a cosmic string. (For subtleties in this interpretation see [27, 28].) The Green functions and the vacuum expectation values of the stress tensor near a straight cosmic string were calculated in [23, 24] and many other papers, including [29, 30, 31, 32, 33, 34, 35, 36, 37, 38, 39, 40].

In addition to moving the focus from wedges to cones, Dowker [21] introduced

a conceptual shift: The infinite-sheeted Riemann surface \mathcal{M}_∞ , previously regarded as a necessary evil required only for irrational cone angles, is now regarded as the fundamental manifold from which the others are built. (See also [41] and references therein.) A θ_1 -periodic image sum (of periodically displaced copies of a Green function on \mathcal{M}_∞) yields the corresponding Green function on \mathcal{M}_{θ_1} , the cone of defining angle θ_1 . This construction (which we discuss in more detail in section 4) is precisely analogous to the creation of Green functions on an interval (or in a rectangular box) as periodic image sums of Green functions on the real line (or a higher-dimensional Euclidean space). A Green function for a wedge is then obtained by one more step of image summation, this time involving a single reflected copy (or, more generally, a sum over some even number of images, including the original source point). In the special case $\theta_1 = 2\pi$, of course, the Green function for Minkowski space is recovered. Although the Green function on \mathcal{M}_∞ is harder to calculate than that on $\mathcal{M}_{2\pi}$ and perhaps not particularly easier than that on a general \mathcal{M}_{θ_1} , the picture in which the covering space \mathcal{M}_∞ is the basic object is nicely consistent with contemporary notions of path integrals (as formal representations of exact solutions) and classical-path sums (as the basic framework for high-frequency and semiclassical approximations). It seems appropriate to refer to \mathcal{M}_∞ (including any extra spatial coordinates such as z in (6)) as the *Dowker manifold* and to the corresponding space-time model as *Dowker space*.

Dowker worked primarily with the same contour-integral representations as Sommerfeld and Carslaw. Our present exposition is strongly influenced by a later paper by Smith [30], which derives the cylinder kernels in total dimensions 3 and 4 without overt use of such complex analysis (“overt” because Smith, and we, freely use special-function identities that appear in standard handbooks without inquiring how they were proved). Formulas in different dimensions are related in a way systematically investigated by Guimarães and Linet [40], which we shall explain in due course. Another method leading to the same results for the cone is that of Helliwell and Konkowski [29], analogous to earlier work for the wedge included in the famous paper [42].

Finally, we must step back to an earlier paper by Lukosz [2], which has been largely overlooked by authors in relativity until recently. This paper deals with the cylinder kernel (and vacuum energy) for a wedge. It is based on an insight similar to Carslaw’s [13, 14]. Lukosz uses the method of images to solve the problem for the very special cases $\theta_0 = \pi/N$, as in section 1.1. He works the solution into a closed form (i.e., one no longer involving a sum over sectors) and then observes that the result satisfies the conditions of the problem for *all* values of θ_0 . His method of course gives also the solution for an arbitrary cone. It can be checked to agree with those of [22, 36, 30], all somewhat differently derived.

Papers continue to be written about vacuum energy in the presence of either wedges or cosmic strings, the scenario being complicated or generalized in various ways of greater or lesser physical importance. An undoubtedly incomplete list is [43, 44, 45, 46, 47, 48, 49, 50, 51, 52, 53, 54, 55]. The most experimentally relevant generalization is to the electromagnetic field, whose study goes back to Deutsch and

Candelas [42] and has been continued in [56, 57, 58, 59] and numerous other references that can be traced back from [58, 59].

2. Formalism in cylindrical coordinates

In order to calculate the vacuum expectation values of all the components of the stress-energy tensor, $T_{\mu\nu}$, we use a different cylinder kernel, \bar{T} , which is an antiderivative of T as defined in section 1.1. \bar{T} satisfies equations (1)–(9) except that (4) is replaced by

$$\frac{\partial \bar{T}}{\partial t}(0, \mathbf{x}, \mathbf{x}') = \delta(\mathbf{x} - \mathbf{x}'). \quad (15)$$

In the calculations that follow, either “0” or an overdot is used to refer to components and derivatives with respect to the physical time coordinate.

The stress-energy tensor formula for a massless real scalar field in flat space is [60]

$$\begin{aligned} T_{\mu\nu} &= \partial_\mu \phi \partial_\nu \phi - \frac{1}{2} \eta_{\mu\nu} \partial^\lambda \phi \partial_\lambda \phi + \xi [\eta_{\mu\nu} \partial_\lambda \partial^\lambda (\phi^2) - \partial_\mu \partial_\nu (\phi^2)] \\ &= \frac{1}{2} \partial_\mu \phi \partial_\nu \phi - \frac{1}{2} \phi \partial_\mu \partial_\nu \phi + \beta [\eta_{\mu\nu} \partial_\lambda \partial^\lambda (\phi^2) - \partial_\mu \partial_\nu (\phi^2)] \end{aligned} \quad (16)$$

in Cartesian coordinates. Here ξ is the usual curvature coupling parameter, but we write $\xi = \beta + \frac{1}{4}$ because then $\beta = 0$ is the algebraically simplest case; thus $\beta = -\frac{1}{4}$ for minimal coupling and $\beta = -\frac{1}{12}$ for conformal coupling in dimension $3 + 1$. In the second version of (16) we have dropped a term that vanishes by virtue of the equation of motion, $\partial_\lambda \partial^\lambda \phi = 0$.

To calculate the components of the tensor in cylindrical coordinates, one can use (16) with η and ∂ reinterpreted as the metric tensor and covariant derivative. Alternatively, one can proceed as Schwartz-Perlov and Olum did for spherical coordinates [60]: Without loss of generality, calculate at a point where the r , θ , and z unit vectors point along the x , y , and z axes. Define the “ \perp ” components of tensors to be along the θ direction, but with respect to an orthonormal basis, so that they have the same physical units as the other components; thus on any scalar function

$$\partial_\perp \phi = \frac{1}{r} \partial_\theta \phi, \quad (17)$$

and in (16) the metric is $\eta_{00} = -1$, $\eta_{rr} = \eta_{\perp\perp} = \eta_{zz} = 1$, all other components 0. The only remaining complication is that in the terms involving second-order derivatives the derivatives of the local basis vectors must be taken into account. That can be done by means of Christoffel symbols as usual in relativity or by direct calculation as in elementary vector calculus, with the results

$$\partial_\perp^2 \phi = \frac{1}{r} \partial_r \phi + \frac{1}{r^2} \partial_\theta^2 \phi \quad (18)$$

and (31). Note also that

$$\partial_\theta^2 (\phi^2) = 2(\partial_\theta \phi)^2 + 2\phi \partial_\theta^2 \phi, \quad (19)$$

so that any one of $\partial_\theta^2 (\phi^2)$, $(\partial_\theta \phi)^2$, and $\phi \partial_\theta^2 \phi$ can be eliminated in favor of the other two. Continuing to follow [60], one then notes that, because of the symmetry of the situation,

the expectation value of ϕ^2 does not depend on time or (in the absence of end plates) the z coordinate, so $\partial_0^2 \langle \phi^2 \rangle = \partial_z^2 \langle \phi^2 \rangle = 0$. For Dowker space or a cone (but not for a wedge) the expectation value of ϕ^2 also does not depend on θ . All these simplifications yield

$$T_{00} = \frac{1}{2}[\dot{\phi}^2 - \phi\ddot{\phi}] - 2\beta[\partial_r(\phi\partial_r\phi) + \frac{1}{r}\phi\partial_r\phi], \quad (20)$$

$$T_{rr} = \frac{1}{2}[(\partial_r\phi)^2 - \phi\partial_r^2\phi] + 2\beta[\frac{1}{r}\phi\partial_r\phi], \quad (21)$$

$$T_{\perp\perp} = \frac{1}{2r^2}Q(\phi) - \frac{1}{2r}\phi\partial_r\phi + 2\beta[\partial_r(\phi\partial_r\phi)], \quad (22)$$

$$T_{zz} = \frac{1}{2}[(\partial_z\phi)^2 - \phi\partial_z^2\phi] + 2\beta[\partial_r(\phi\partial_r\phi) + \frac{1}{r}\phi\partial_r\phi], \quad (23)$$

where

$$Q(\phi) = (\partial_\theta\phi)^2 - \phi\partial_\theta^2\phi = 2(\partial_\theta\phi)^2 - \frac{1}{2}\partial_\theta^2(\phi^2). \quad (24)$$

Now we can rewrite the components of $T_{\mu\nu}$ in terms of the cylinder kernel, \bar{T} , rather than ϕ . Since $\langle 0|\phi(x)\phi(x')|0\rangle = -\frac{1}{2}\bar{T}(x, x')$, we have, for example,

$$\langle \phi\partial_r\phi \rangle = -\frac{1}{2}\partial_r\bar{T}, \quad \langle \phi\partial_r^2\phi \rangle = -\frac{1}{2}\partial_r^2\bar{T}, \quad \langle (\partial_r\phi)^2 \rangle = -\frac{1}{2}\partial_r\partial_r\bar{T}, \quad (25)$$

where x' is set equal to x after differentiation. (Strictly speaking, we should symmetrize $2\partial_r^2$ as $\partial_r^2 + \partial_r'^2$, etc., but it can be seen that this does not matter.) The derivatives for the other coordinates are computed similarly. The components of $T_{\mu\nu}$ finally become

$$\langle T_{00} \rangle = -\frac{1}{2}\partial_t^2\bar{T} + \beta[\partial_r\partial_r'\bar{T} + \partial_r^2\bar{T} + \frac{1}{r}\partial_r\bar{T}] \quad (26)$$

$$\langle T_{rr} \rangle = -\frac{1}{4}[\partial_r\partial_r'\bar{T} - \partial_r^2\bar{T}] - \frac{1}{r}\beta\partial_r\bar{T}, \quad (27)$$

$$\langle T_{\perp\perp} \rangle = \frac{1}{4r}\partial_r\bar{T} + \frac{1}{4r^2}[\partial_\theta^2\bar{T} - \partial_\theta\partial_\theta'\bar{T}] - \beta[\partial_r\partial_r'\bar{T} + \partial_r\bar{T}] \quad (\text{general}) \quad (28)$$

$$= \frac{1}{4r}\partial_r\bar{T} + \frac{1}{2r^2}\partial_\theta^2\bar{T} - \beta[\partial_r\partial_r'\bar{T} + \partial_r\bar{T}] \quad (\text{symmetric case}), \quad (29)$$

$$\langle T_{zz} \rangle = -\frac{1}{4}[\partial_z\partial_z'\bar{T} - \partial_z^2\bar{T}] - \beta[\partial_r\partial_r'\bar{T} + \partial_r^2\bar{T} + \frac{1}{r}\partial_r\bar{T}]. \quad (30)$$

Henceforth the expectation-value brackets around components of the stress tensor will be omitted for simplicity of notation; and later the notation $T_{\mu\nu}$ will be abused once again after a vacuum subtraction. Again in these equations it is understood that formally the two space-time points are set equal after the differentiations. In reality these diagonal values are divergent, and either the points must be kept separated until after a vacuum subtraction has been performed, or some other kind of regularization must be adopted.

In the interior of a wedge it is possible for $T_{r\perp}$ to have a nonzero vacuum expectation value, but we shall not consider that component of the tensor further in this paper except to record the needed formula

$$\partial_\perp\partial_\parallel\phi = \partial_\parallel\partial_\perp\phi = \frac{1}{r}\partial_r\partial_\theta\phi - \frac{1}{r^2}\partial_\theta\phi. \quad (31)$$

Here, to prevent ambiguity we write ∂_\parallel for the radial covariant derivative. (When it stands alone, ∂_\parallel is equivalent to ∂_r : $\partial_\parallel^2\phi = \partial_r^2\phi$, for instance.)

3. Calculation of \bar{T}

We now consider the problem of calculating cylinder kernels in polar coordinates. Various methods can be used. Guided by physical motivations, Smith [30] used one method in three (total) dimensions and a different one in four. We have carried out both calculations in both ways, and here we demonstrate how to do the four-dimensional case each way, to stress that they are mathematically interchangeable. Finally, we summarize the three-dimensional results and describe how adjacent dimensions are related.

3.1. Homogeneous boundary-value problem; r - θ - z expansion

The first method is to solve the boundary-value problem set up in section 1 (or its modification by (15)). Thus \bar{T} satisfies for $t > 0$ the homogeneous 4-dimensional Laplace equation,

$$\frac{\partial^2 T}{\partial t^2} + \frac{\partial^2 T}{\partial r^2} + \frac{1}{r} \frac{\partial T}{\partial r} + \frac{1}{r^2} \frac{\partial^2 T}{\partial \theta^2} + \frac{\partial^2 T}{\partial z^2} = 0, \quad (32)$$

along with a periodicity condition, $T(\theta + \theta_1) = T(\theta)$, and the initial condition

$$T(0, \mathbf{r}, \mathbf{r}') = \frac{1}{r} \delta(r - r') \delta(\theta - \theta') \delta(z - z'). \quad (33)$$

Expanding T in a Fourier series in θ yields

$$T(t, r, \theta, z) = \sum_{n=-\infty}^{\infty} e^{in\theta(\frac{2\pi}{\theta_1})} T_n(t, r, z) \quad (34)$$

with

$$T_n(t, r, z) = \frac{1}{\theta_1} \int_0^{\theta_1} e^{-in\theta(\frac{2\pi}{\theta_1})} T(t, r, \theta, z) d\theta. \quad (35)$$

Using these expressions in (32), we see that

$$\frac{\partial^2 T_n}{\partial t^2} + \frac{\partial^2 T_n}{\partial r^2} + \frac{1}{r} \frac{\partial T_n}{\partial r} - \frac{n^2}{r^2} \left(\frac{2\pi}{\theta_1}\right)^2 T_n + \frac{\partial^2 T_n}{\partial z^2} = 0. \quad (36)$$

From (33) and (35) we obtain

$$\begin{aligned} T_n(0, r, z) &= \frac{1}{\theta_1} \int_0^{\theta_1} d\theta e^{-in\theta(\frac{2\pi}{\theta_1})} \frac{1}{r} \delta(r - r') \delta(\theta - \theta') \delta(z - z') \\ &= \frac{1}{\theta_1} e^{-in\theta'(\frac{2\pi}{\theta_1})} \frac{1}{r} \delta(r - r') \delta(z - z'). \end{aligned} \quad (37)$$

We now make a further step of variable separation, $T_{\text{sep}}(t, r) = T(t)R(r)Z(z)$, and we define $\lambda = \frac{2n\pi}{\theta_1}$ and occasionally suppress “ n ” in the notation. From (36) we get

$$\frac{T''}{T} + \frac{R''}{R} + \frac{Z''}{Z} + \frac{1}{r} \frac{R'}{R} - \frac{\lambda^2}{r^2} = 0. \quad (38)$$

We let

$$-\frac{T''}{T} - \frac{Z''}{Z} = \frac{R''}{R} + \frac{1}{r} \frac{R'}{R} - \frac{\lambda^2}{r^2} = -\omega^2, \quad (39)$$

and therefore conclude that

$$R'' + \frac{1}{r}R' + \left(\omega^2 - \frac{\lambda^2}{r^2}\right)R = 0, \quad (40)$$

$$Z = e^{ikz}, \quad T = e^{-\omega't}, \quad \omega'^2 \equiv \omega^2 + k^2. \quad (41)$$

The appropriate solution of (40) is the Bessel function $J_{|\lambda|}(\omega r)$ (and not $Y_{|\lambda|}(\omega r)$ because of the minimal irregularity at $r = 0$). Now we can define the combined Bessel and Fourier transform

$$T_n(t, r, z) = \int_0^\infty \omega d\omega \int_{-\infty}^\infty dk \tilde{T}(\omega, k) J_{|\lambda|}(\omega r) e^{-\omega't} e^{ikz}. \quad (42)$$

When $t = 0$, from (37) we get

$$T_n(0, r, z) = \frac{e^{-i\lambda\theta'} \delta(r - r') \delta(z - z')}{\theta_1 r} \equiv P(r, z), \quad (43)$$

and from (42) we see that

$$T_n(0, r, z) = \int_0^\infty \omega d\omega \int_{-\infty}^\infty dk \tilde{T}(\omega, k) J_{|\lambda|}(\omega r) e^{ikz}. \quad (44)$$

Therefore we can solve for $\tilde{T}(\omega, k)$:

$$\begin{aligned} \tilde{T}(\omega, k) &= \frac{1}{2\pi} \int_{-\infty}^\infty dz \int_0^\infty r dr J_{|\lambda|}(\omega r) P(r, z) e^{-ikz} \\ &= \frac{e^{-i\lambda\theta'}}{2\pi\theta_1} J_{|\lambda|}(\omega r') e^{-ikz'}. \end{aligned} \quad (45)$$

From this one finally gets

$$T(t, r, \theta, z) = \int_0^\infty \omega d\omega \int_{-\infty}^\infty dk \sum_{n=-\infty}^\infty \tilde{T}_n(\omega, k) J_{|\lambda|}(\omega r) e^{in\theta} e^{-\omega't} e^{ikz} \quad (46)$$

or, in full glory,

$$\begin{aligned} T(t, r, \theta, z, r', \theta', z') &= \frac{1}{2\pi\theta_1} \sum_{n=-\infty}^\infty \int_0^\infty \omega d\omega \int_{-\infty}^\infty dk J_{|\lambda|}(\omega r) J_{|\lambda|}(\omega r') \\ &\quad \times e^{i\lambda(\theta-\theta')} e^{-\omega't} e^{ik(z-z')}. \end{aligned} \quad (47)$$

The formula for \bar{T} is the same as for T except for a factor $-\omega'$ in the denominator to implement the integration with respect to t :

$$\begin{aligned} \bar{T}(t, r, \theta, z, r', \theta', z') &= -\frac{1}{\pi\theta_1} \sum_{n=-\infty}^\infty e^{i\lambda(\theta-\theta')} \int_0^\infty \omega d\omega J_{|\lambda|}(\omega r) J_{|\lambda|}(\omega r') \\ &\quad \times \int_{-\infty}^\infty dk (\omega^2 + k^2)^{-1/2} e^{-t\sqrt{\omega^2+k^2}} e^{ik(z-z')}. \end{aligned} \quad (48)$$

By [61, (3.961.2)] the k integral equals $2K_0(\omega\zeta)$, where $\zeta = \sqrt{t^2 + (z - z')^2}$. Hence we have

$$\bar{T}(t, r, \theta, z, r', \theta', z') = -\frac{1}{\pi\theta_1} \sum_{n=-\infty}^\infty e^{i\lambda(\theta-\theta')} \int_0^\infty \omega d\omega J_{|\lambda|}(\omega r) J_{|\lambda|}(\omega r') K_0(\omega\zeta). \quad (49)$$

The integral over ω can be computed [61, (6.522.3)], giving us the Fourier-series representation of \bar{T} ,

$$\bar{T}(t, r, \theta, z, r', \theta', z') = -\frac{1}{\pi\theta_1} \sum_{n=-\infty}^{\infty} e^{i\lambda(\theta-\theta')} \frac{1}{r_1 r_2} \left(\frac{r_2 - r_1}{r_2 + r_1} \right)^{|n|}, \quad (50)$$

where $r_1 \equiv \sqrt{(r - r')^2 + \zeta^2}$ and $r_2 \equiv \sqrt{(r + r')^2 + \zeta^2}$. Let

$$\frac{r_2 - r_1}{r_2 + r_1} \equiv e^{-u}. \quad (51)$$

Smith [30] points out the alternative formulas for u that we present in section 4 and sums the series to get the final closed form of \bar{T} ,

$$\begin{aligned} \bar{T}(t, r, \theta, z, r', \theta', z') &= -\frac{1}{2\pi\theta_1 r r' \sinh u} \sum_{n=-\infty}^{\infty} e^{-|\lambda|u + i\lambda(\theta-\theta')} \\ &= -\frac{1}{2\pi\theta_1 r r' \sinh u} \frac{\sinh(\frac{2\pi}{\theta_1} u)}{\cosh(\frac{2\pi}{\theta_1} u) - \cos \frac{2\pi}{\theta_1} (\theta - \theta')}. \end{aligned} \quad (52)$$

(Actually, Smith calculated the Wightman function (a Green function for the wave equation) rather than \bar{T} . It differs only by replacing t^2 by $-(x^0 - x^0')^2$.)

3.2. Nonhomogeneous problem; t - θ - z expansion

The second method was employed by Smith [30] in dimension 3. In our case (dimension 4) it starts by observing that \bar{T} (extended evenly in t) satisfies the nonhomogeneous Green-function equation

$$\frac{\partial^2 \bar{T}}{\partial t^2} + \frac{\partial^2 \bar{T}}{\partial r^2} + \frac{1}{r} \frac{\partial \bar{T}}{\partial r} + \frac{1}{r^2} \frac{\partial^2 \bar{T}}{\partial \theta^2} + \frac{\partial^2 \bar{T}}{\partial z^2} = \frac{2}{r} \delta(t) \delta(r - r') \delta(\theta - \theta') \delta(z - z'). \quad (53)$$

in all of \mathbf{R}^4 . The proof of (53) is a standard application of Green's identity combined with an image construction in the t direction [62].

To solve (53) we again use a Fourier decomposition in θ ,

$$\bar{T}(t, r, \theta, z) = \sum_{n=-\infty}^{\infty} e^{in\theta(\frac{2\pi}{\theta_1})} T_n(t, r, z), \quad (54)$$

$$T_n(t, r, z) = \frac{1}{\theta_1} \int_0^{\theta_1} e^{-in\theta(\frac{2\pi}{\theta_1})} \bar{T}(t, r, \theta, z). \quad (55)$$

Again let $\lambda = \frac{2n\pi}{\theta_1}$, and without loss of generality take $\theta' = 0$ and $z' = 0$. By substituting into (53), we get

$$\frac{\partial^2 T_n}{\partial t^2} + \frac{\partial^2 T_n}{\partial r^2} + \frac{1}{r} \frac{\partial T_n}{\partial r} - \frac{\lambda^2}{r^2} T_n + \frac{\partial^2 T_n}{\partial z^2} = \frac{2}{\theta_1 r} \delta(t) \delta(r - r') \delta(z). \quad (56)$$

The delta functions in z and t can be represented as

$$\delta(z - z') = \frac{2}{\pi} \int_0^\infty dk \cos kz \cos kz', \quad (57)$$

$$\delta(t - t') = \frac{2}{\pi} \int_0^\infty d\omega' \cos \omega' t \cos \omega' t', \quad (58)$$

so we get

$$\tilde{T}_n(\omega', r, k) = \int_0^\infty dt' \cos(\omega't') \int_0^\infty dz' \cos(kz') T_n(t', r, z'), \quad (59)$$

$$T_n(t, r, z) = \frac{2}{\pi} \int_0^\infty d\omega' \cos(\omega't) \frac{2}{\pi} \int_0^\infty dk \cos(kz) \tilde{T}_n(\omega', r, k). \quad (60)$$

Consequently, (56) becomes

$$-(\omega'^2 + k^2)\tilde{T}_n + \frac{\partial^2 \tilde{T}_n}{\partial r^2} + \frac{1}{r} \frac{\partial \tilde{T}_n}{\partial r} - \frac{\lambda^2}{r^2} \tilde{T}_n = \frac{2}{\theta_1 r} \delta(r - r'). \quad (61)$$

Let $\omega^2 = \omega'^2 + k^2$ (not the same relation as in (41)!). The solution of (61) has the form

$$\tilde{T}_n = \begin{cases} C_\omega I_{|\lambda|}(\omega r) & \text{for } r < r', \\ D_\omega K_{|\lambda|}(\omega r) & \text{for } r > r'. \end{cases} \quad (62)$$

From the continuity and jump conditions implementing the delta function in (61), we get that

$$C_\omega = -\frac{2}{\theta_1} K_{|\lambda|}(\omega r'), \quad D_\omega = -\frac{2}{\theta_1} I_{|\lambda|}(\omega r'). \quad (63)$$

Therefore,

$$\tilde{T}_n(\omega, r) = -\frac{2}{\theta_1} I_{|\lambda|}(\omega r_{<}) K_{|\lambda|}(\omega r_{>}), \quad (64)$$

and we get

$$\begin{aligned} \bar{T}(t, r, \theta, z) &= -\frac{2}{\pi^2 \theta_1} \sum_{n=-\infty}^{\infty} e^{in\theta(\frac{2\pi}{\theta_1})} \\ &\quad \times \int_0^\infty dk \int_0^\infty d\omega' \cos(\omega't) \cos(kz) I_{|\lambda|}(\omega r_{<}) K_{|\lambda|}(\omega r_{>}). \end{aligned} \quad (65)$$

Since $2\omega' d\omega' = 2\omega d\omega$ and $\omega' = 0$ when $\omega = k$, the formula can be rewritten

$$\begin{aligned} \bar{T}(t, r, \theta, z) &= -\frac{2}{\pi^2 \theta_1} \sum_{n=-\infty}^{\infty} e^{in\theta(\frac{2\pi}{\theta_1})} \int_0^\infty \omega d\omega I_{|\lambda|}(\omega r_{<}) K_{|\lambda|}(\omega r_{>}) \\ &\quad \times \int_0^\omega dk \frac{\cos((\omega^2 - k^2)^{\frac{1}{2}} t) \cos(kz)}{(\omega^2 - k^2)^{\frac{1}{2}}}. \end{aligned} \quad (66)$$

The k integral yields $\frac{\pi}{2} J_0(\omega\zeta)$, where $\zeta \equiv \sqrt{z^2 + t^2}$ [61, (3.876.7)]. Thus by [61, (6.578.11)]

$$\begin{aligned} \bar{T}(t, r, \theta, z) &= -\frac{1}{\pi \theta_1} \sum_{n=-\infty}^{\infty} e^{in\theta(\frac{2\pi}{\theta_1})} \int_0^\infty \omega d\omega I_{|\lambda|}(\omega r_{<}) K_{|\lambda|}(\omega r_{>}) J_0(\omega\zeta) \\ &= -\frac{1}{\pi \theta_1} \sum_{n=-\infty}^{\infty} e^{in\theta(\frac{2\pi}{\theta_1})} \times \frac{e^{-i\pi/2} Q_{|\lambda|-\frac{1}{2}}^{\frac{1}{2}}(\cosh u)}{\sqrt{2\pi} rr' (\sinh u)^{\frac{1}{2}}}, \end{aligned} \quad (67)$$

where

$$\cosh u \equiv \frac{r^2 + r'^2 + z^2 + t^2}{2rr'}$$

and [61, (8.754.4)]

$$Q_{|\lambda|-\frac{1}{2}}^{\frac{1}{2}}(\cosh u) = i\sqrt{\frac{\pi}{2\sinh u}}e^{-|\lambda|u}.$$

Therefore,

$$\bar{T}(t, r, \theta, z) = -\frac{1}{2\pi\theta_1 r r' \sinh u} \sum_{n=-\infty}^{\infty} e^{i\lambda\theta - |\lambda|u},$$

which agrees with the previous result (52).

Remark: Several other variations are possible (see [63] for the 3-dimensional analogs). One can solve (53) by a complete Fourier analysis in all variables; then whether the first or second method above develops depends on whether the first integral one evaluates is over the variable ω' conjugate to t or the variable ω conjugate to r . Yet another approach [42, 29] is to introduce an additional “proper time” coordinate and find a Fourier solution for the corresponding heat kernel or propagator; then integrating over the proper time segues back to the approach just described, but evaluating the ω' integral first yields a different representation.

3.3. Three-dimensional problem; positive mass

Both methods described above can be used in three dimensions, yielding the equivalent results [30]

$$T(t, r, r', \theta) = \frac{1}{\theta_1} \sum_{n=-\infty}^{\infty} e^{i\lambda\theta} \frac{1}{\sqrt{r r'}} Q_{|\lambda|-\frac{1}{2}}(\cosh u_0) \quad (68)$$

$$= -\frac{1}{\pi\theta_1 \sqrt{2r r'}} \int_{u_0}^{\infty} du \frac{1}{\sqrt{\cosh u - \cosh u_0}} \frac{\sinh(\frac{2\pi}{\theta_1} u)}{\cosh(\frac{2\pi}{\theta_1} u) - \cos(\frac{2\pi\theta}{\theta_1})}. \quad (69)$$

Here

$$\cosh u_0 = \frac{r^2 + r'^2 + t^2}{2r r'}, \quad \lambda = \frac{2n\pi}{\theta_1}, \quad (70)$$

and Q is a second-kind Legendre function. For details see [30, 64].

Formulas (68) and (69) cannot be simplified into an elementary closed form like (52) (just as a circular Bessel function is not elementary, but a spherical Bessel function is). However, (69) clearly is related to (52); indeed, the former is a certain integral transform of the latter. To understand fully the relations between cylinder kernels in different dimensions, it is necessary to enlarge the discussion to allow the scalar field to have a mass [40]. That is, a term $m^2 T$ is added to the right side of (2). In the case of two spatial dimensions, this would lead via (11) to the equation

$$\left(\frac{\partial^2}{\partial t^2} + \frac{\partial^2}{\partial r^2} + \frac{1}{r} \frac{\partial}{\partial r} + \frac{1}{r^2} \frac{\partial}{\partial \theta^2} - m^2 \right) T = 0 \quad (71)$$

(or the corresponding equation for \bar{T} , or a similar nonhomogeneous equation like (53)). But if we merely rename m as k , (53) is recognized as the result of Fourier-transforming in z the four-dimensional massless field equation with spatial operator (7). Because we

are working in Euclidean signature when we study cylinder kernels, a massive Klein–Gordon equation is the same thing as a Helmholtz equation in one higher dimension.

It follows that by taking a Fourier transform of a massive cylinder kernel with respect to the mass, one obtains a cylinder kernel for the massless theory in one higher dimension. (The massive higher-dimensional case can be reached by using only a piece of the lower-dimensional mass in the transform [40, (2.5)].) Conversely, by Fourier-transforming the four-dimensional \bar{T} (52) in z , and then setting the Fourier variable equal to zero, one obtains the three-dimensional massless \bar{T} ; and (69) can be interpreted in this light after a change of variable from z to u (using (74), for example).

4. The vacuum in periodic spaces

In summary, we have (in total dimension 4) for the cone with angular periodicity θ_1

$$\bar{T}_{\theta_1}(t, r, r', \theta, z) = -\frac{1}{2\pi\theta_1 r r' \sinh u} \frac{\sinh\left(\frac{2\pi u}{\theta_1}\right)}{\cosh\left(\frac{2\pi u}{\theta_1}\right) - \cos\left(\frac{2\pi\theta}{\theta_1}\right)}, \quad (72)$$

where u is defined by any of the equivalent formulas

$$u = -\ln \frac{r_2 - r_1}{r_2 + r_1}, \quad (73)$$

$$r_1 = \sqrt{(r - r')^2 + z^2 + t^2}, \quad r_2 = \sqrt{(r + r')^2 + z^2 + t^2};$$

$$2rr' \cosh u = r^2 + r'^2 + z^2 + t^2; \quad (74)$$

$$2rr' \sinh u = \sqrt{[r^2 + r'^2 + z^2 + t^2]^2 - 4r^2 r'^2}; \quad (75)$$

$$4rr' \sinh^2\left(\frac{u}{2}\right) = (r - r')^2 + z^2 + t^2. \quad (76)$$

(Without loss of generality we have set t' , z' , and θ' equal to 0. When derivatives with respect to primed coordinates are needed, one simply replaces z by $z - z'$, etc., first.)

When $\theta_1 = 2\pi$, (72) reduces to the formula for Minkowski space in cylindrical coordinates,

$$\bar{T}_{2\pi} = -\frac{1}{4\pi^2 r r'} \frac{1}{\cosh u - \cos \theta} \quad (77)$$

$$= -\frac{1}{2\pi^2 (r^2 + r'^2 + t^2 + z^2 - 2rr' \cos(\theta))}. \quad (78)$$

(The two forms are shown equivalent by (74) and the law of cosines.) When $\theta_1 \rightarrow \infty$, (72) becomes the formula for the infinite-sheeted Dowker space-time,

$$\bar{T}_{\infty} = -\frac{1}{2\pi^2 r r' \sinh u} \frac{u}{u^2 + \theta^2}. \quad (79)$$

\bar{T}_{θ_1} can be recovered from \bar{T}_{∞} as a periodic image sum: after suppressing the irrelevant coordinates,

$$\bar{T}_{\theta_1}(\theta - \theta') = \sum_{n=-\infty}^{\infty} \bar{T}_{\infty}(\theta - \theta' + n\theta_1). \quad (80)$$

In particular,

$$\bar{T}_{2\pi}(\theta - \theta') = \sum_{n=-\infty}^{\infty} \bar{T}_{\infty}(\theta - \theta' + 2\pi n). \quad (81)$$

In terms of normal modes, $\bar{T}_{2\pi}$ is a sum over angular momentum quantum number, while \bar{T}_{∞} is an integral over angular momentum. \bar{T}_{∞} can be found by separation of variables (integration over modes) in a slight variation of the calculation in the previous section. Formula (80) can be verified, or discovered, in *Mathematica* or by complex analysis; indeed, the entire theory of vacuum stress in cones and wedges could be developed from formula (79) in this way. The Dowker Green function \bar{T}_{∞} is physically the most elementary; it tells how to diffract a path off the isolated conical singularity. The additional effects of periodicity, and hence of reflecting wedge walls, can be obtained from \bar{T}_{∞} by images, or summation over paths, appropriate to each geometry in question. Of course, these remarks extend to the energy density and the rest of the stress tensor, and also to other Green functions, not just the cylinder kernel.

The sum (80) has a structure similar to the formula for \bar{T} in a universe that is periodic in one direction with period L_1 :

$$\bar{T}_{L_1}(x - x') = \sum_{n=-\infty}^{\infty} \bar{T}_0(x - x' + nL_1). \quad (82)$$

Again, \bar{T}_{L_1} is a Fourier sum, \bar{T}_0 a Fourier integral. The algebra leading from (79) to (72) according to (80) is very similar to that leading from (13) to a closed form for (82).

There is, of course, a major glitch in the analogy of \bar{T}_{∞} and \bar{T}_{θ_1} to \bar{T}_0 and \bar{T}_{L_1} , respectively: it is $\bar{T}_{2\pi}$ (not \bar{T}_{∞}) that, like \bar{T}_0 , is the free-space Green function that gives the zero-point energy density that must be subtracted from the energy of any other configuration. A periodic space has nontrivial Casimir energy, inherent in \bar{T}_{L_1} after the subtraction. In the early stages of the universe, this vacuum energy should affect the cosmological expansion.

Actually, this last conclusion is not universally accepted. The critique runs somewhat as follows: A real physicist is interested in the scalar field only as a model of the electromagnetic field. The (experimentally verified) electromagnetic Casimir energy is the energy of interaction of fluctuations of the electrons in the bounding conductors (the long-range limit of the van der Waals force). The field energy is just a bookkeeping device. But in a periodic universe (or a higher-dimensional closed universe) there are no boundaries, no fluctuating electrons. There is no experimental evidence that cosmological vacuum energy exists. (The observed dark energy may have something to do with zero-point energy, despite the notorious factor 10^{120} , but it has nothing to do (in the absence of small extra dimensions, at least [65]) with the renormalized Casimir energy, which has a rest frame and is unobservably small at the present epoch.)

Nevertheless, the mathematics (and indirectly confirmed physics) of quantum field theory unambiguously says that the vacuum energy density of a periodic universe differs from that of infinite space by a locally finite amount in precise analogy to how the vacuum energy density of infinite space (looked at in polar coordinates) differs from

that of Dowker space. In each case the increment is the difference between a Fourier series and a Fourier integral over the same spectral integrand. If you believe in the stress tensor of quantum field theory, this picture is totally consistent and unsurprising (except for the enduring mystery of what happens to the zero-point energy). But if you don't, you are forced into an untenable position:

- To calculate vacuum energy in the periodic universe, you must ignore the (mathematically appropriate) Fourier sum in favor of the integral (since you don't believe vacuum energy can exist in the absence of van der Waals sources).
- In polar coordinates, you must use the sum to get the right answer for empty Euclidean space. The integral gives something else, the energy density of the Dowker manifold.

We see no possibility of a theoretical justification for this ad hoc switch of point of view. (Of course, this is not the same as an experimental or observational verification of the theory.)

5. Numerics

We now present some vacuum energy calculations for various cone and wedge spaces, based on the cylinder kernel for a cone as given in (72) and alternatively in (80), and executed in *Mathematica*. Most of these results were previously presented in [66].

In this section we will work on diagonal, with $r' = r$, $z = 0$, and $\theta = 0$, but with $t > 0$. This is the traditional exponential ultraviolet cutoff. For flat space, we have

$$T_{00} = \frac{3}{2\pi^2 t^4}, \quad T_{rr} = T_{\perp\perp} = T_{zz} = \frac{1}{2\pi^2 t^4}, \quad (83)$$

and of course we expect to subtract this “zero-point stress” from the stress tensor in any other configuration to get a physically meaningful quantity; this has been done in all the plots below, and in (84). Because $t^4 T_{\mu\nu}$ (with $z = 0$) depends on r and t only in the ratio r/t , the plot for $t = 1$ actually serves for all positive values of t , as the axis labels indicate.

In the plots, solid curves are for the ultraviolet cutoff $t \neq 0$ and dashed curves are for $t = 0$. When the cutoff is thus removed, the energy density and pressures are finite at each point in the interior of Ω but (usually) develop nonintegrable singularities at the boundaries ($\theta \rightarrow 0$, $\theta \rightarrow \theta_0$, or $r \rightarrow 0$). Note that when a cutoff is present ($t > 0$), the key quantity u is strictly positive even when all the coordinates are on diagonal ($r = r'$, $z = z' = 0$, $\theta = \theta' = 0$); therefore, all the quantities being plotted remain finite at the wedge plates, although the plots may give the impression of vertical asymptotes there.

When multiple traces are shown in the same panel, blue, red, and (when present) yellow curves correspond to the cases in the order listed in the caption. To facilitate viewing on a monochrome device, we indicate in each case whether the corresponding ordering is from top to bottom or bottom to top in the bulk of the figure. Also, multiple plots within one figure are sometimes plotted with different horizontal and vertical scales,

in order to better show the behavior of the functions. In many cases, the energy density has been replotted in a separate graph to show the behavior for small r more clearly.

Plots of the energy density and pressure in the Dowker space with $\beta = 0$ ($\xi = \frac{1}{4}$), obtained from (79), are given in figure 1. Figure 2 displays the additional terms in the energy density and pressure when $\beta \neq 0$. Because these correction terms are proportional to $\beta \equiv \xi - \frac{1}{4}$, it suffices to plot the case $\beta = 1$.

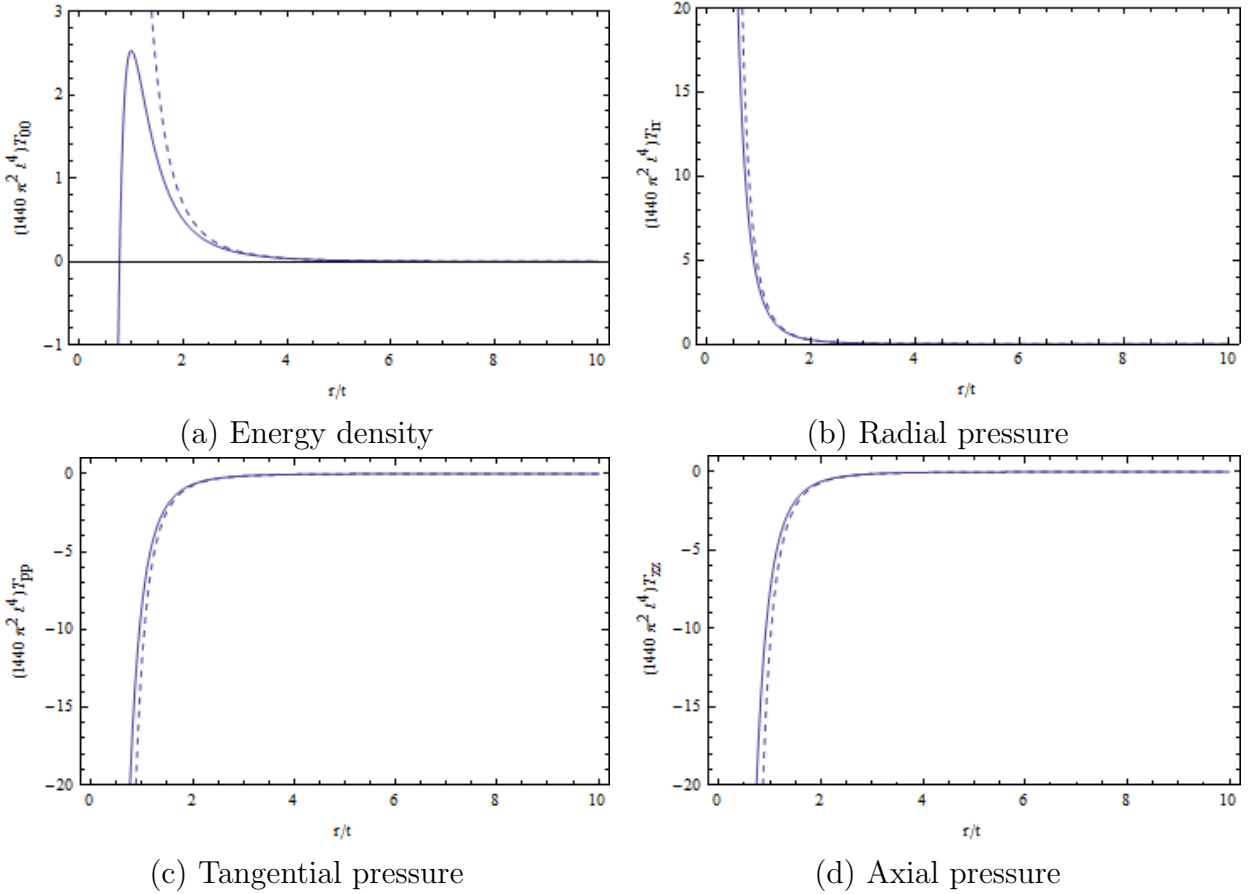


Figure 1. Plot of the Dowker energy density and pressure as a function of r with $\xi = \frac{1}{4}$.

In figures 3 and 4 the energy density and pressure are presented for cone spaces with various cone angles. Notice that the overall sign of the energy density function changes at $\theta_1 = 2\pi$. Plots for $\theta_1 = 10000\pi$ match very well with plots for Dowker space, as expected since Dowker space is the large-period limit of the cones. The behavior of the energy density near $r = 0$ is illustrated in figure 5.

The curvature-coupling correction terms to the energy density and pressure are presented in figures 6 and 7 for various cone angles. The energy density for the conformal case, where $\xi = 1/6$, is plotted in figure 8 and compared with the case $\xi = 1/4$.

In figures 9 and 10 we present the energy density and pressure for the cone space, and the correction terms, as functions of the cone size θ_1 with fixed $r = 1$.

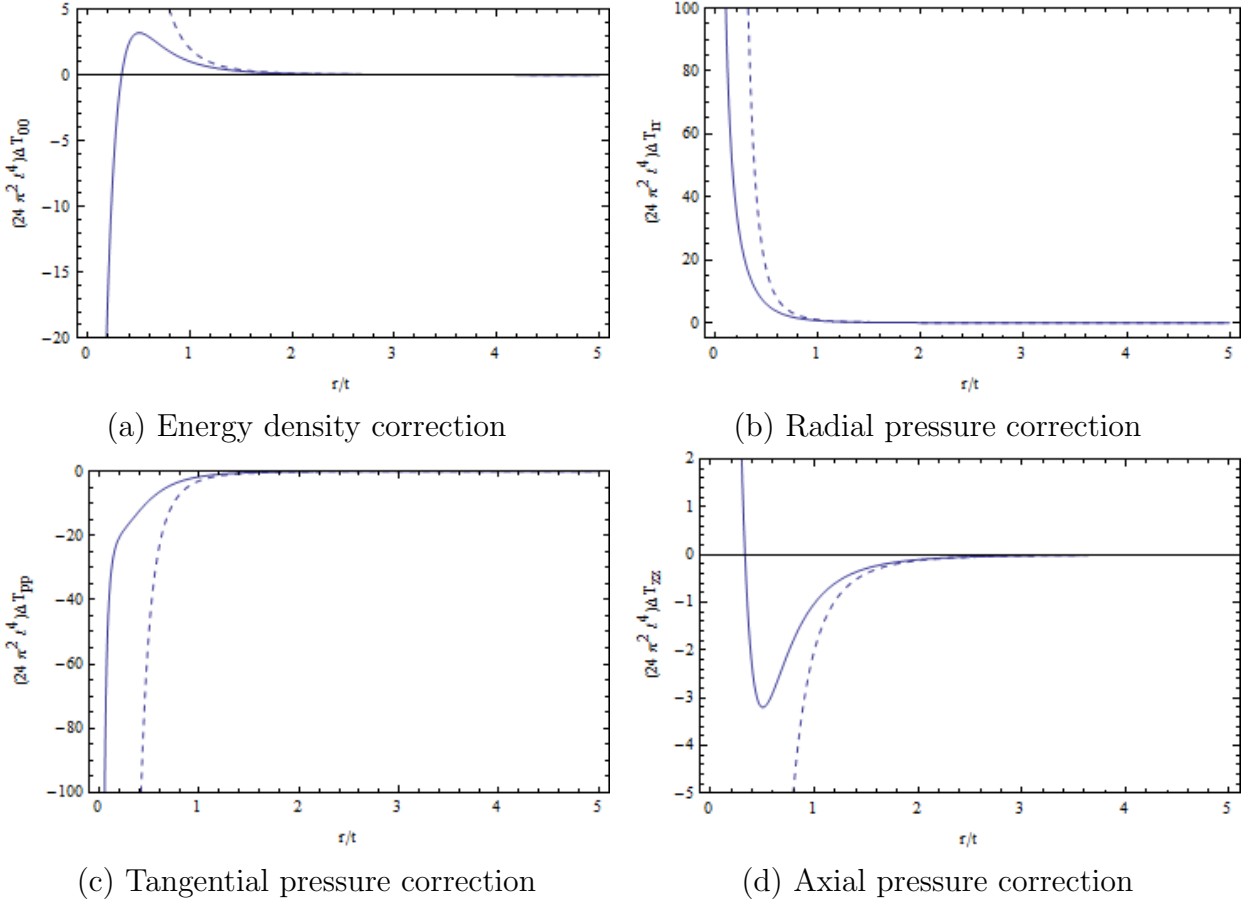


Figure 2. Plot of the Dowker energy density and pressure curvature-coupling corrections as a function of r with $\beta = 1$.

For a Dirichlet wedge with opening angle θ_0 , we have an infinite sum over positive and negative images in Dowker space, and the resulting expression for \bar{T} is

$$\begin{aligned}
 & - \frac{1}{4\pi\theta_0 r r'} \sinh(u) \left(\frac{\sinh(\pi u/\theta_0)}{\cosh(\pi u/\theta_0) - \cos(\pi(\theta - \theta')/\theta_0)} \right. \\
 & \quad \left. - \frac{\sinh(\pi u/\theta_0)}{\cosh(\pi u/\theta_0) - \cos(\pi(\theta + \theta')/\theta_0)} \right) \\
 & + \frac{1}{4\pi^2 r r'} \frac{1}{\cosh u - \cos \theta}. \tag{84}
 \end{aligned}$$

The energy density now becomes a function of θ as well as r . Figures 11 and 12 show the energy density as a function of θ for various values of ξ , θ_0 , and r . Figures 11(b) and 12(b) show that when the cutoff is removed, the conformal energy density is independent of the angle (a fortiori, not divergent at the wedge plates), but at finite cutoff the function deviates strongly from this limiting behavior near the boundary. Both panels of figure 11 show that the cutoff function is very far from the limit function when r is rather small. Figures 13 and 14 show that the energy density remains finite at the boundaries. Figures 15 and 16 show the energy density as a function of r for various values of ξ , θ_0 ,

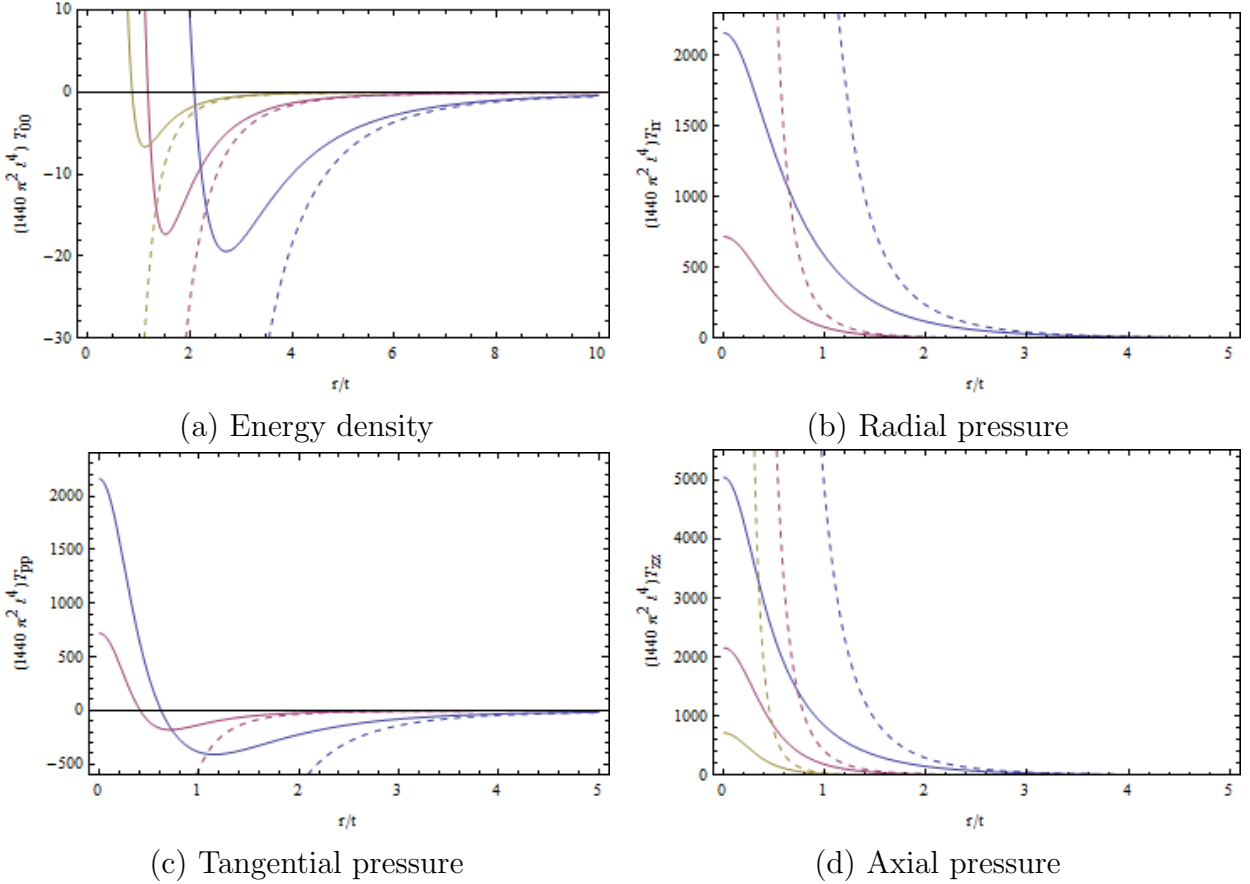


Figure 3. Energy density and pressure for $\xi = 1/4$ and cone angles $\theta_1 = \pi/4, \pi/2,$ and π (respectively blue, red, yellow, bottom to top in (a) and (c), and top to bottom in (b) and (d)). (Some plots for $\theta_1 = \pi$ are missing because of a numerical problem.)

and θ .

Numerically, there is no qualitative difference between “good” and “bad” wedge angles, despite the great difference between them with regard to solvability by the classic method of images. The exception is the case $\theta_0 = \pi$ (for which the “cone” is flat space), where the “wedge” energy is just that of a single reflecting plane, expressed in polar coordinates.

6. Conclusions and outlook

There is a dual relationship between infinite (Euclidean) space and finite flat space (a circle or torus): Green functions for the infinite case can be obtained from the finite case by taking a limit, in which a Fourier series becomes a Fourier transform, or the finite, periodic case can be obtained from the infinite one as an infinite sum over image sources. A similar relationship exists in a two-dimensional space that is locally flat except at a single conical singularity (hence in a higher-dimensional space with a singular axis), except that the Fourier analysis is now with respect to the angular coordinate. The

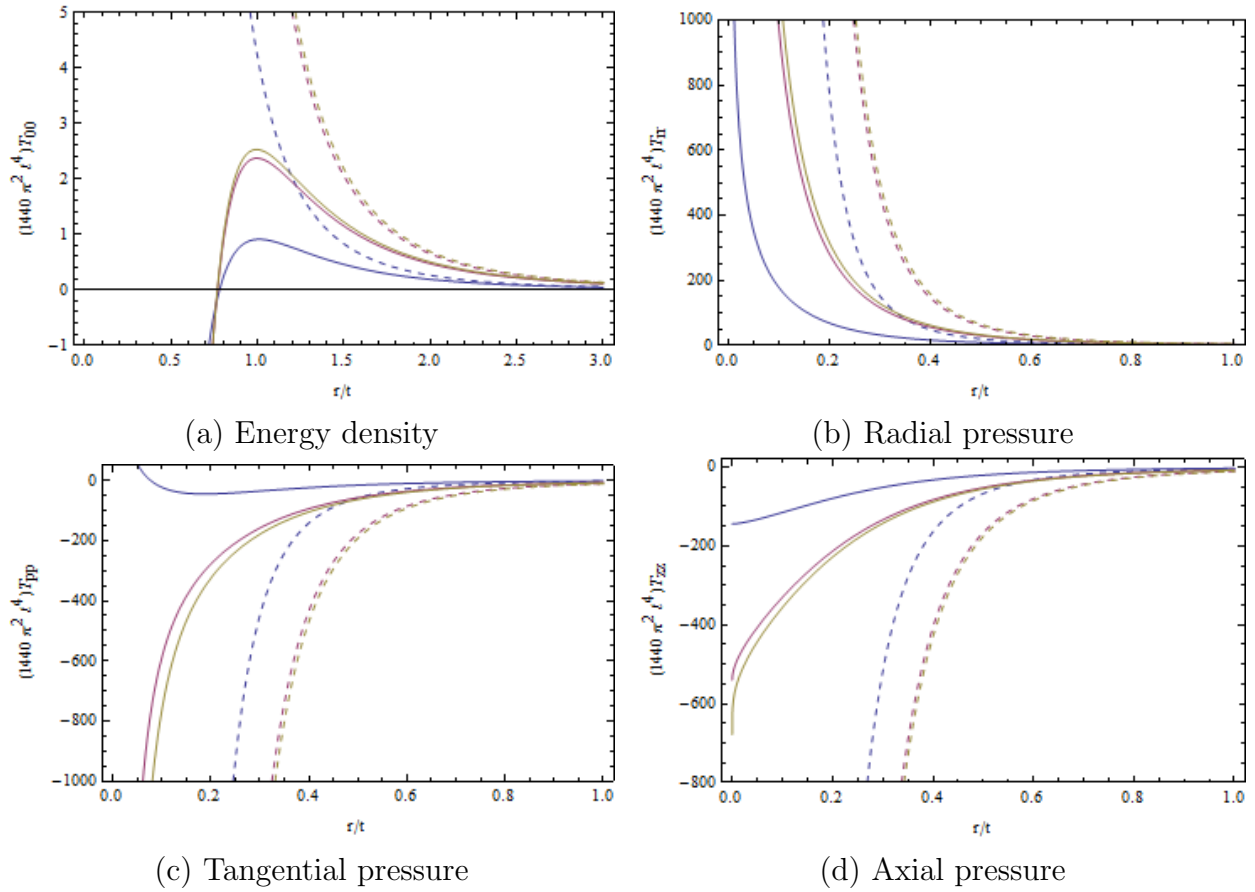


Figure 4. Energy density and pressure for $\xi = 1/4$ and cone angles $\theta_1 = 2.5\pi, 8\pi,$ and 10000π (respectively blue, red, yellow, bottom to top in (a) and (b), and top to bottom in (c) and (d)).

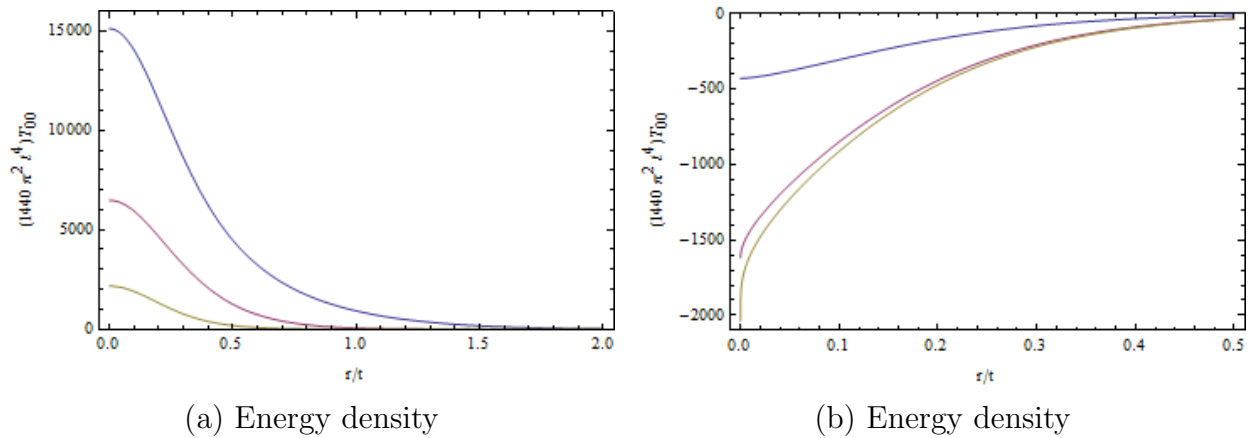


Figure 5. Energy density for $\xi = 1/4$ and cone angles (a) $\theta_1 = \pi/4, \pi/2,$ and π (respectively blue, red, yellow, top to bottom), and (b) $\theta_1 = 2.5\pi, 8\pi,$ and 10000π (top to bottom). Behavior near $r = 0$.

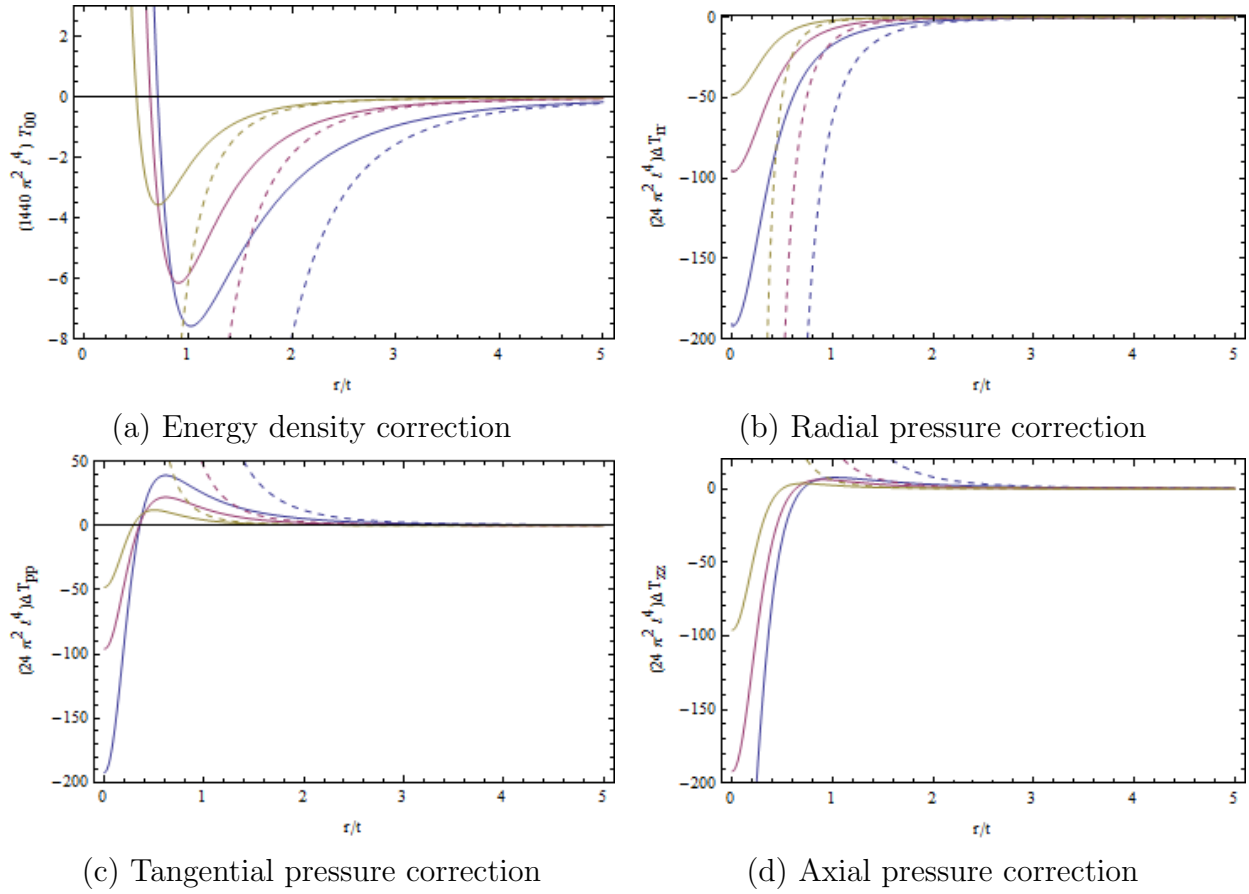


Figure 6. Energy density and pressure correction terms for $\beta = 1$ and cone angles $\theta_1 = \pi/4, \pi/2,$ and π (bottom to top).

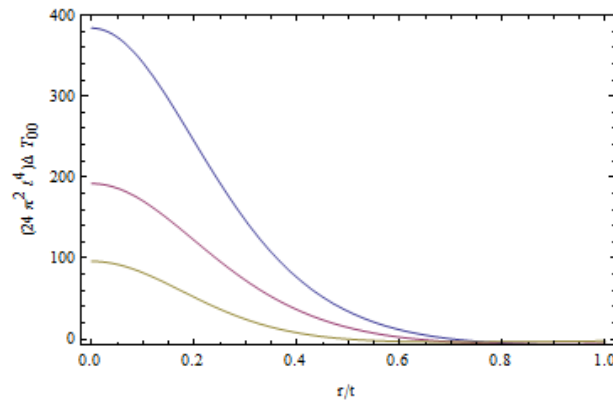


Figure 7. Energy density correction term for $\beta = 1$ and cone angles $\theta_1 = \pi/4, \pi/2,$ and π (top to bottom). Behavior near $r = 0$.

role of the infinite space is now played by an infinite-sheeted singular surface, whose importance has been particularly stressed by Dowker. Among the continuum of periodic factor spaces (cones) of the Dowker manifold with respect to periodic image sums, one

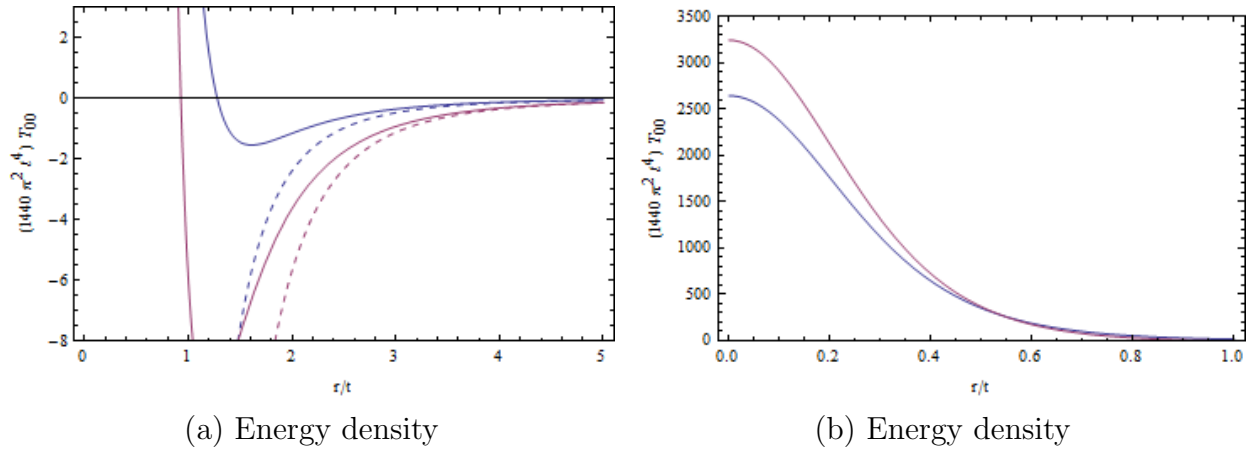


Figure 8. Energy density for $\xi = 1/6$ and $\xi = 1/4$ (top to bottom in (a), and bottom to top in (b)), with cone angle $\theta_1 = 0.8\pi$. Behavior near $r = 0$ is shown in (b).

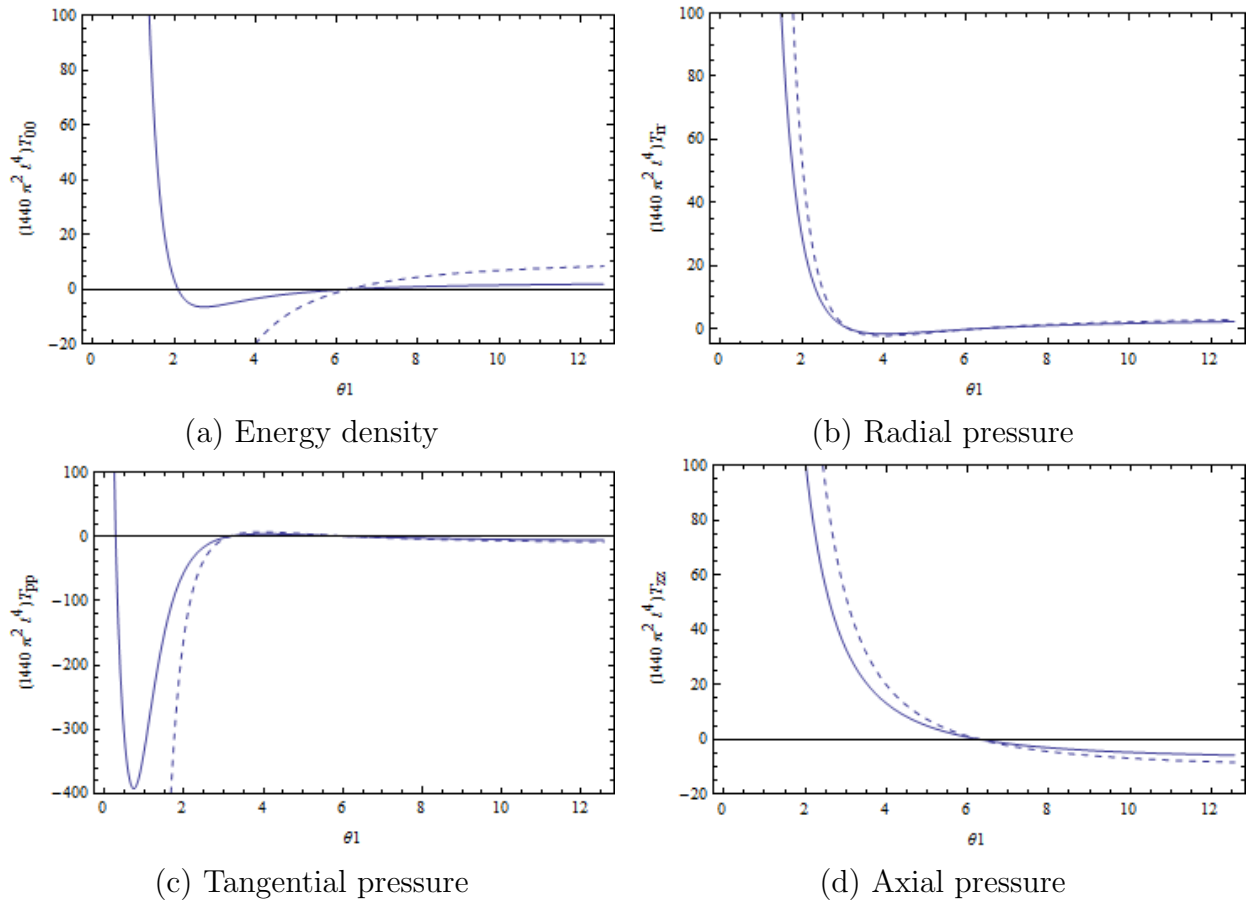


Figure 9. Energy density and pressure for the cone space as a function of θ_1 , with $\beta = 0$ and $r = 1$.

is our familiar, nonsingular Euclidean space. From the cone of arbitrary angle a further image sum, with respect to a single reflection, yields the Green functions for a perfectly

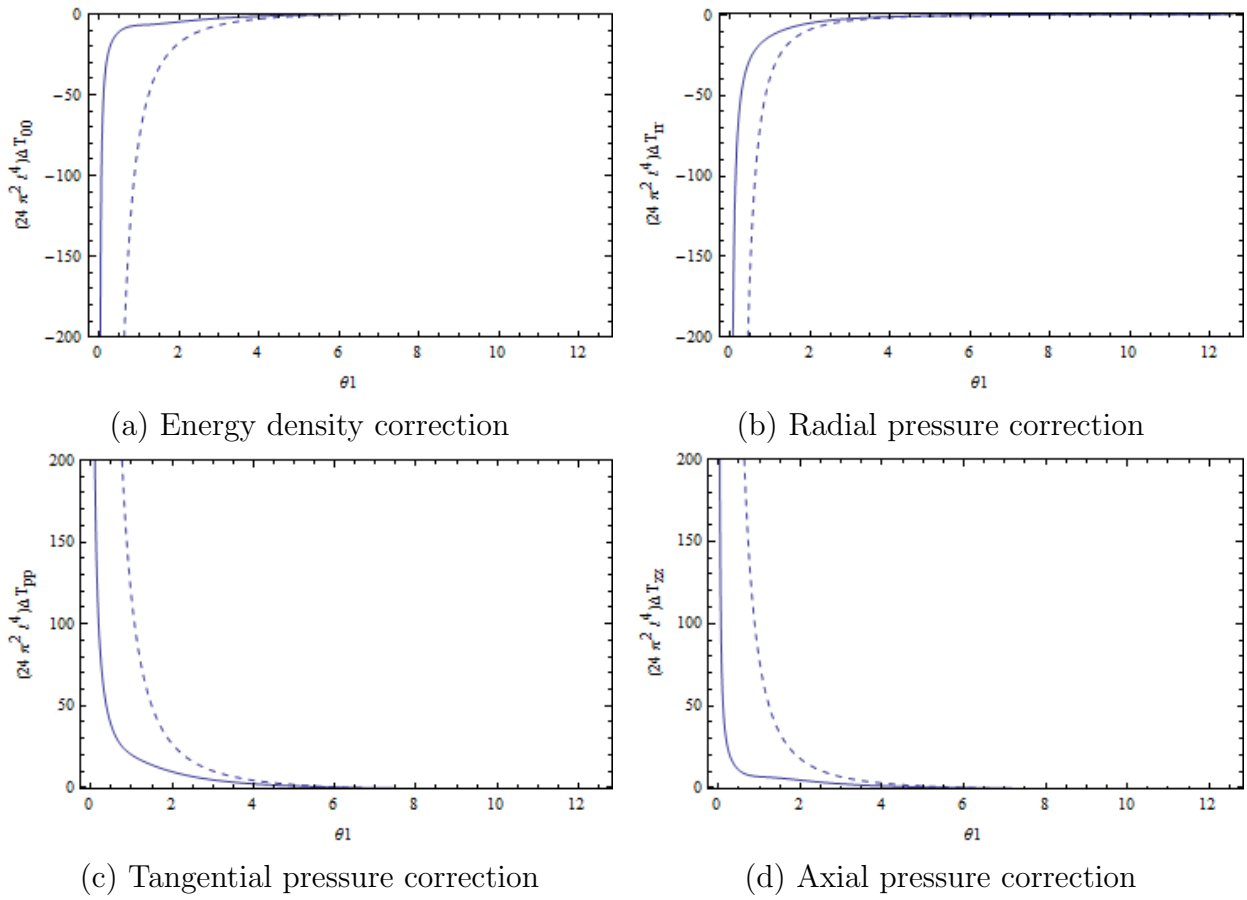


Figure 10. Energy density and pressure curvature-coupling corrections for the cone space as a function of θ_1 , with $r = 1$.

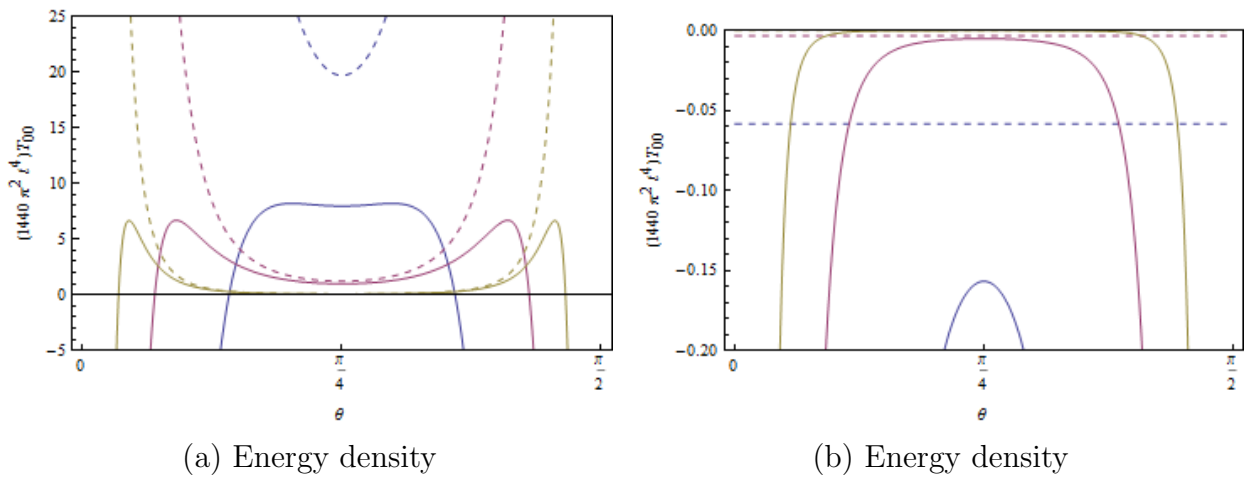


Figure 11. Energy density in a wedge as a function of θ with $\theta_0 = \pi/2$ and (a) $\xi = 1/4$, for r at 2, 4, and 8 (top to bottom); (b) $\xi = 1/6$, for r at 4, 8, and 16 (bottom to top).

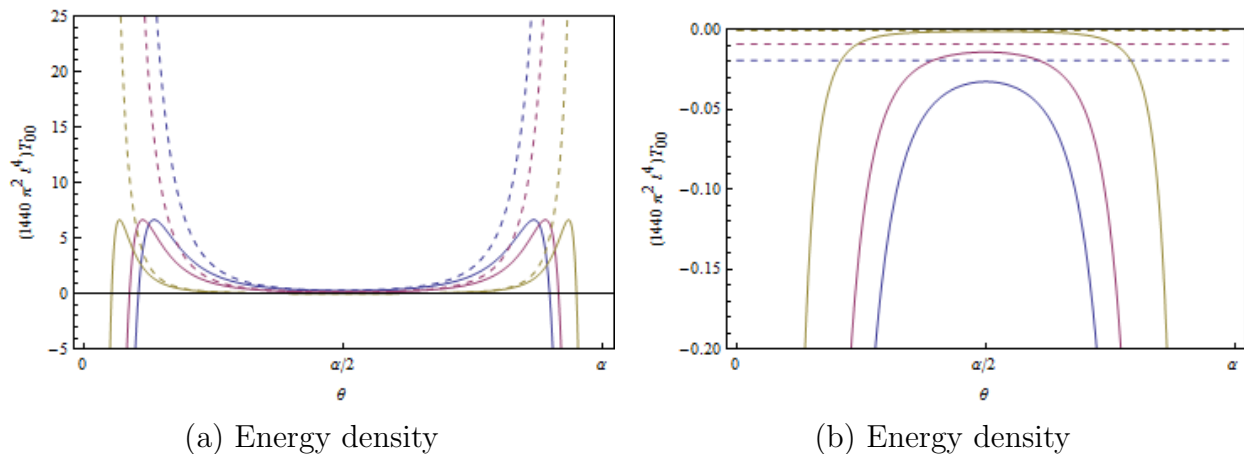


Figure 12. Wedge energy density as a function of θ with $r = 8$ and θ_0 values $\pi/3$, $2\pi/5$, and $2\pi/3$ for (a) $\xi = 1/4$ (top to bottom); (b) $\xi = 1/6$ (bottom to top).

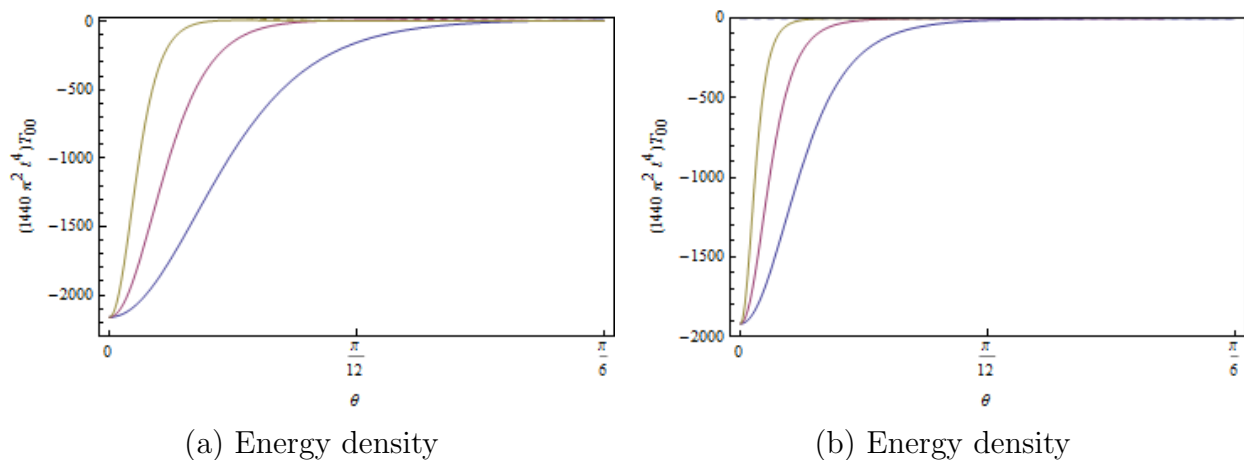


Figure 13. Wedge energy density as a function of θ with $\theta_0 = \pi/2$ and (a) $\xi = 1/4$, for r at 2, 4, and 8 (bottom to top); (b) $\xi = 1/6$, for r at 4, 8, and 16 (bottom to top). Behavior near $\theta = 0$.

reflecting wedge in Euclidean space, with an arbitrary opening angle.

As shown by Lukosz and Smith, the particular Green function that is most useful for calculating the vacuum expectation value of the stress tensor in scalar quantum field theory can be found in closed form by rather elementary methods in all these spaces — Dowker space, cones, and wedges. The vacuum energy density (and pressure) in such systems consists of three components: the effect of the central singularity present already in the Dowker space, the effect of periodicity associated with a cone, and the specific effect of the reflecting edges of the wedge. The first two of these are independent of the angular coordinate inside the wedge. From this point of view, Euclidean space is itself a cone, whose periodicity energy precisely cancels the energy of the (erstwhile) central singularity. This periodicity energy is closely analogous to that of a torus relative to infinite space, which has sometimes been questioned because of the absence of sources.

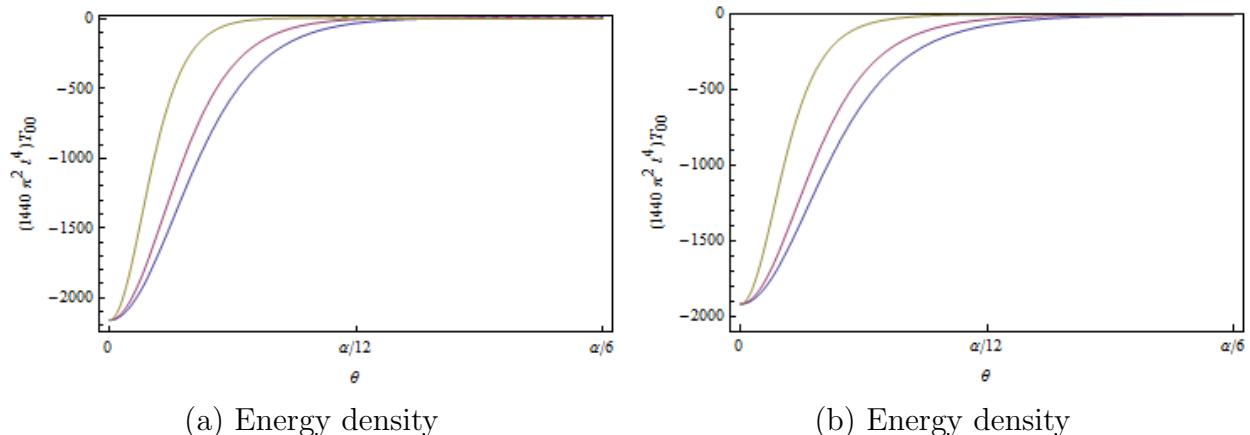


Figure 14. Wedge energy density as a function of θ with $r = 8$ and θ_0 values $\pi/3$, $2\pi/5$, and $2\pi/3$ for (a) $\xi = 1/4$ (bottom to top); (b) $\xi = 1/6$ (bottom to top). Behavior near $\theta = 0$.

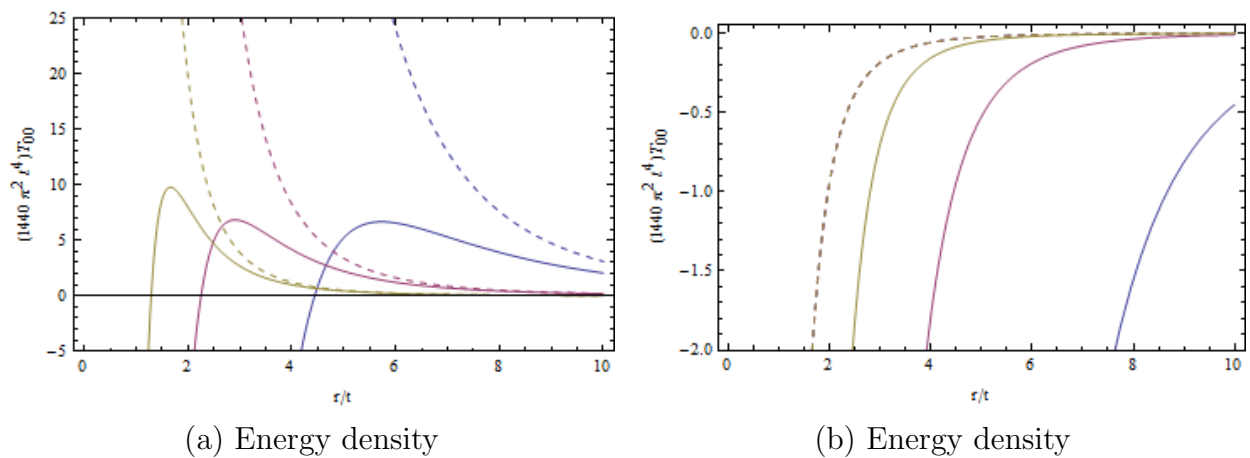


Figure 15. Wedge energy density as a function of r with $\theta_0 = \pi/2$ and θ values $\pi/16$, $\pi/8$, and $\pi/4$ for (a) $\xi = 1/4$ (top to bottom); (b) $\xi = 1/6$ (bottom to top).

We have presented numerous plots of the (renormalized) energy density and pressures in these systems, both with and without an exponential ultraviolet cutoff. In some circumstances a cutoff can be regarded as a mathematical device that can be completely removed at the end. However, alternatively a finite cutoff can be viewed as a small step toward a realistic physical model of the boundary material. In that case the standards for physical acceptability of the renormalized cutoff stress tensor are higher. Recent work on plane boundaries [67, 68] indicates that the exponential cutoff introduces unphysical behavior in the energy density (but not the pressure) very near the boundary, and suggests that a better model of both energy and pressure could be obtained by replacing that cutoff (which corresponds to a separation of the arguments of the Green function in the imaginary time direction) by a point separation in a “neutral” direction. In the present cylindrical situation that would mean a separation in the axial

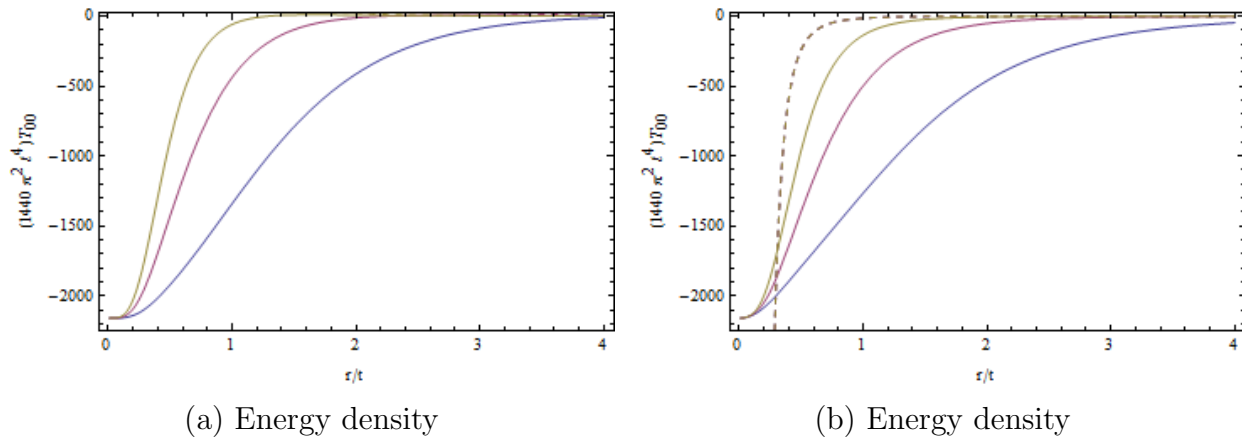


Figure 16. Wedge energy density as a function of r with $\theta_0 = \pi/2$ and θ values $\pi/16$, $\pi/8$, and $\pi/4$ for (a) $\xi = 1/4$ (bottom to top); (b) $\xi = 1/6$ (bottom to top). Behavior near $r = 0$.

direction, and that prescription is currently under investigation, starting in [66].

Acknowledgments

We are grateful to the editors of this Dowkerfest volume for the invitation to write this article, and to the organizers of the Miltonfest conference in Norman, Oklahoma, in 2010 for the opportunity to present a preliminary account there. As a corollary, we are ever grateful to Stuart Dowker and Kim Milton for their inspiration and counsel. We thank R. Jackiw and F. D. Mera for comments. This work was supported by NSF Grants PHY-0554849 and PHY-0968269 and by a one-semester postdoctoral appointment for J. Wagner in the Texas A&M Mathematics Department.

References

- [1] Lukosz W 1973 Electromagnetic zero-point energy shift induced by conducting surfaces *Z. Physik* **258** 99–107
- [2] Lukosz W 1973 Electromagnetic zero-point energy shift induced by conducting surfaces. II *Z. Physik* **262** 327–348
- [3] Bender C M and Hays P 1976 Zero-point energy of fields in a finite volume *Phys. Rev. D* **14** 2622–2632
- [4] Fulling S A 2003 Systematics of the relationship between vacuum energy calculations and heat-kernel coefficients *J. Phys. A* **36** 6857–6873
- [5] Meixner J 1949 Die Kantenbedingung in der Theorie der Beugung elektromagnetischer Wellen an vollkommen leitenden ebenen Schirmen *Ann. Physik* **6** 2-9
- [6] Kay B S and Studer U M 1991 Boundary conditions for quantum mechanics on cones and fields around cosmic strings *Commun. Math. Phys.* **139** 103-139
- [7] Sommerfeld A 1896 Mathematische Theorie der Diffraction *Math. Ann.* **47** 317–374
- [8] Sommerfeld A 1897 Über verzweigte Potentiale im Raum *Proc. London Math. Soc.* **28** 395–429
- [9] Sommerfeld A 1901 Theoretisches über die Beugung der Röntgenstrahlen *Zeitschr. Mat. Physik* **46** 11–97

- [10] Sommerfeld A 1935 Theorie der Beugung, *Die Differential- und Integralgleichungen der Mechanik und Physik* Vol. 2 ed P Frank and R von Mises (Braunschweig:Vieweg and New York:Rosenberg (1943)), pp 808–875
- [11] Sommerfeld A 2004 *Mathematical Theory of Diffraction* translated and annotated by R. J. Nagem, M. Zampolli and G. Sandri (Boston:Birkhäuser).
- [12] Carslaw H S 1899 Some multiform solutions of the partial differential equations of physical mathematics and their applications *Proc. London Math. Soc.* **30** 121–163
- [13] Carslaw H S 1910 The Green's function for a wedge of any angle, and other problems in the conduction of heat *Proc. London Math. Soc.* **8** 365–374
- [14] Carslaw H S 1920 Diffraction of waves by a wedge of any angle *Proc. London Math. Soc.* **18** 291–306
- [15] Reiche F 1912 Die Beugung des Lichtes an einem ebene, rechteckigen Keil von unendlicher Leitfähigkeit *Ann. Physik* **342** 131–156
- [16] Wiegrefe A 1912 Über einige mehrwertige Lösungen der Wellengleichung $\Delta u + k^2 u = 0$ und ihre Anwendung in der Beugungstheorie *Ann. Physik* **344** 449–484
- [17] Oberhettinger F 1954 Diffraction of waves by a wedge *Commun. Pure Appl. Math.* **7** 551–563
- [18] Deser S and Jackiw R 1988 Classical and quantum scattering on a cone *Commun. Math. Phys.* **118** 495–509
- [19] De Sousa Gerbert P and Jackiw R 1989 Classical and quantum scattering on a spinning cone *Commun. Math. Phys.* **124** 229–260
- [20] Sieber M, Pavloff N and Schmidt C 1997 Uniform approximation for diffractive contributions to the trace formula in billiard systems *Phys. Rev. E* **55** 2279–2299
- [21] Dowker J S 1977 Quantum field theory on a cone *J. Phys. A* **10** 115–124
- [22] Dowker J S 1978 Thermal properties of Green's functions in Rindler, de Sitter, and Schwarzschild spaces *Phys. Rev. D* **18** 1856–1860
- [23] Dowker J S 1987 Casimir effect around a cone *Phys. Rev. D* **36** 3095–3101
- [24] Dowker J S 1987 Vacuum averages for arbitrary spin around a cosmic string *Phys. Rev. D* **36** 3742–3746
- [25] Dowker J S 1990 Quantum field theory around conical defects *The Formation and Evolution of Cosmic Strings* ed G Gibbons, S Hawking and T Vachaspati (Cambridge: Cambridge), pp. 251–261
- [26] Fulling S A and Ruijsenaars S M N 1987 Temperature, periodicity, and horizons *Phys. Reports* **152** 135–176
- [27] Geroch R and Traschen J 1987 Strings and other distributional sources in general relativity *Phys. Rev. D* **36** 1017–1031
- [28] Futamase T and Garfinkle D 1988 What is the relation between $\Delta\phi$ and μ for a cosmic string? *Phys. Rev. D* **37** 2086–2091
- [29] Helliwell T M and Konkowski D A 1986 Vacuum fluctuations outside cosmic strings *Phys. Rev. D* **34** 1918–1920
- [30] Smith A G 1990 Gravitational effects of an infinite straight cosmic string on classical and quantum fields: Self-forces and vacuum fluctuations *The Formation and Evolution of Cosmic Strings*, ed G Gibbons, S Hawking and T Vachaspati (Cambridge:Cambridge), pp 263–292
- [31] Frolov V P and Serebriany E M 1987 Vacuum polarization in the gravitational field of a cosmic string *Phys. Rev. D* **35** 3779–3782
- [32] Frolov V P, Pinzul A and Zelnikov A I 1995 Vacuum polarization at finite temperature on a cone *Phys. Rev. D* **51** 2770–2774
- [33] Parker L 1987 Gravitational particle production in the formation of cosmic strings *Phys. Rev. Lett.* **59** 1369–1372
- [34] Davies P C W and Sahni V 1988 Quantum gravitational effects near cosmic strings *Class. Quantum Grav.* **5** 1–17
- [35] Shiraishi K and Hirenzaki S 1992 Quantum aspects of self-interacting fields around cosmic strings

- Class. Quantum Grav.* **9** 2277–2286
- [36] Linet B 1987 Quantum field theory in the space-time of a cosmic string *Phys. Rev. D* **35** 536–539
- [37] Linet B 1992 The Euclidean thermal Green function in the spacetime of a cosmic string *Class. Quantum Grav.* **9** 2429–2436
- [38] Linet B 1995 Euclidean spinor Green's functions in the space-time of a straight cosmic string *J. Math. Phys.* **36** 3694–3703
- [39] Linet B 1996 Euclidean thermal spinor Green's function in the spacetime of a straight cosmic string *Class. Quantum Grav.* **13** 97–103
- [40] Guimarães M E X and Linet B 1994 Scalar Green's functions in an Euclidean space with a conical-type line singularity *Commun. Math. Phys.* **165** 297–310
- [41] Ziolkowski R W 1986 A path-integral-Riemann-space approach to the electromagnetic wedge diffraction problem *J. Math. Phys.* **27** 2271–2281
- [42] Deutsch D and Candelas P 1979 Boundary effects in quantum field theory *Phys. Rev. D* **20** 3063–3080
- [43] Parker L 1987 Gravitational particle production in the formation of cosmic strings *Phys. Rev. Lett* **59** 1369–1372
- [44] Bordag M 1990 On the vacuum-interaction of two parallel cosmic strings *Ann. Physik* **47** 93–100
- [45] Guimarães M E X 1995 Vacuum polarization at finite temperature around a magnetic flux cosmic string *Class. Quantum Grav.* **12** 1705–1713
- [46] Khusnutdinov N R and Bezerra V B 2001 Self-energy and self-force in the space-time of a thick cosmic string *Phys. Rev. D* **64** 083506
- [47] Rezaeian A H and Saharian A A 2002 Local Casimir energy for a wedge with a circular outer boundary *Class. Quantum Grav.* **19** 3625–3634
- [48] Saharian A A and Tarloyan A S 2005 Wightman function and scalar Casimir densities for a wedge with a cylindrical boundary *J. Phys. A* **38** 8763–8780
- [49] Bezerra de Mello E R, Bezerra V B, Saharian A A and Tarloyan A S 2006 Vacuum polarization induced by a cylindrical boundary in the cosmic string spacetime *Phys. Rev. D* **74** 025017
- [50] Bezerra de Mello E R, Bezerra V B and Saharian A A 2007 Electromagnetic Casimir densities induced by a conducting cylindrical shell in the cosmic string spacetime *Phys. Lett. B* **645** 245–254
- [51] Bezerra de Mello E R and Saharian A A 2012 Topological Casimir effect in compactified cosmic string spacetime *Class. Quantum Grav.* **29** 035006
- [52] Ottewill A C and Taylor P 2010 Vacuum polarization on the Schwarzschild metric threaded by a cosmic string *Phys. Rev. D* **82** 104013
- [53] Sitenko Yu A and Vlasii N D 2012 Induced vacuum energy-momentum tensor in the background of a cosmic string *Class. Quantum Grav.* **29** 095002
- [54] Milton K A, Wagner J and Kirsten K 2009 Casimir effect for a semitransparent wedge and an annular piston *Phys. Rev. D* **80** 125028
- [55] Dowker J S 2011 Spherical Casimir pistons *Class. Quantum Grav.* **28** 155018
- [56] Brevik I and Lygren M 1996 Casimir effect for a perfectly conducting wedge *Ann. Phys.* **251** 157–179
- [57] Nesterenko V V, Lambiase G and Scarpetta G 2002 Casimir effect for a perfectly conducting wedge in terms of local zeta function *Ann. Phys.* **298** 403–420
- [58] Brevik I, Ellingsen S Å and Milton K A 2009 Electromagnetic Casimir effect in a medium-filled wedge *Phys. Rev. E* **79** 041120
- [59] Ellingsen S Å, Brevik I and Milton K A 2009 Electromagnetic Casimir effect in a medium-filled wedge. II *Phys. Rev. E* **80** 021125
- [60] Schwartz-Perlov D and Olum K D 2005 Energy conditions for a generally coupled scalar field outside a reflecting sphere *Phys. Rev. D* **72** 165013
- [61] Gradshteyn I S and Ryzhik I M 1980 *Table of Integrals, Series, and Products* (New York:Academic)
- [62] Fulling S A 2008 Preliminaries to numerical analysis of cylinder kernels (unpublished notes)

- <http://www.math.tamu.edu/~fulling/sphere/prenum.pdf>
- [63] Fulling S A 2008 Two-dimensional Euclidean Helliwell–Konkowski calculation (unpublished notes) <http://www.math.tamu.edu/~fulling/qvac08/truong/ehk.pdf>
- [64] Truong P N 2008 (untitled unpublished notes) <http://www.math.tamu.edu/~fulling/qvac08/truong/ckpc.pdf> and <http://www.math.tamu.edu/~fulling/qvac08/truong/tft3d.pdf>
- [65] Milton K A, Kantowski R, Kao C and Wang Y 2001 Constraints on extra dimensions from cosmological and terrestria measurements *Mod. Phys. Lett. A* **16** 2281–2289
- [66] Trendafilova C S 2012 Vacuum Energy for Static, Cylindrically Symmetric Systems, Undergraduate Research Fellow thesis, Texas A&M University
- [67] Fulling S A 2010 Vacuum energy density and pressure near boundaries (QFExt09), *Internat. J. Mod. Phys.* **25** 2364–2372
- [68] Fulling S A, Milton K A and Wagner J 2012 Energy density and pressure in power-wall models (QFExt11), *Internat. J. Mod. Phys. Conf. Ser.*, to appear